The Abdus Salam
International Centre for Theoretical Physics

United Nations
Educational, Scientific
and Cultural Organization

International Atomic
Energy Agency

SMR.1738 - 24

WINTER COLLEGE
on
QUANTUM AND CLASSICAL ASPECTS
of
INFORMATION OPTICS

30 January - 10 February 2006

DIGITAL IMAGING:

DIGITAL HOLOGRAPHY AND DIGITAL IMAGE PROCESSING

L. P. YAROSLAVSKY

Faculty of Engineering
Tel Aviv University
Dept. of Interdisciplinary Studies
Tel Aviv 69978
Israel

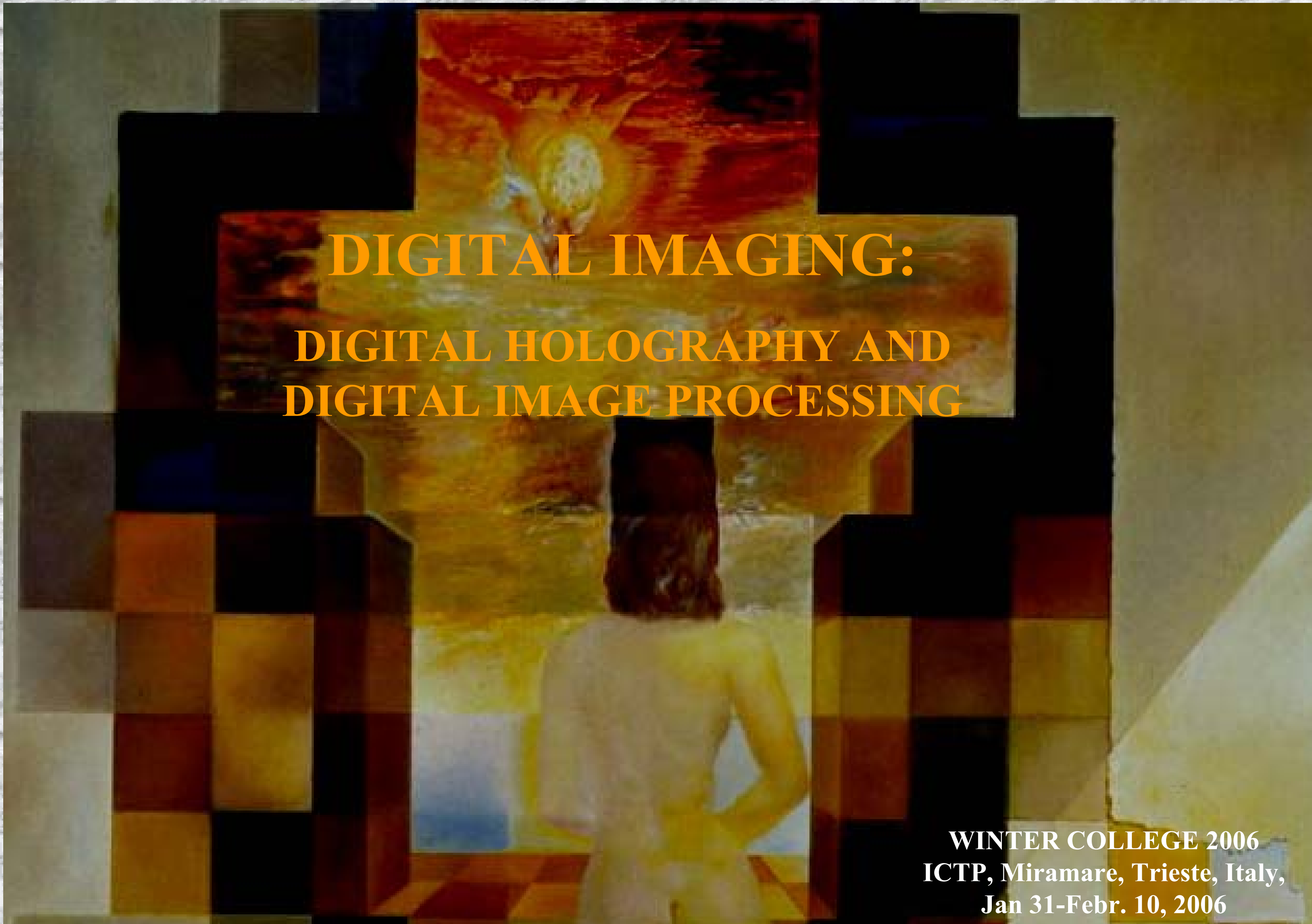
DIGITAL IMAGING:
DIGITAL HOLOGRAPHY AND
DIGITAL IMAGE PROCESSING
WINTER COLLEGE 2006
ICTP, Miramare, Trieste, Italy,
Jan 31-Febr. 10, 2006

Digital holography and image processing: twins born by the computer era

Digital holography:

- computer synthesis, analysis and simulation of wave fields

Digital image processing:

- digital image formation;
- image perfection;
- image enhancement for visual analysis;
- image measurements and parameter estimation;
- image storage & transmission;
- image visualization

DIGITAL HOLOGRAPHY:

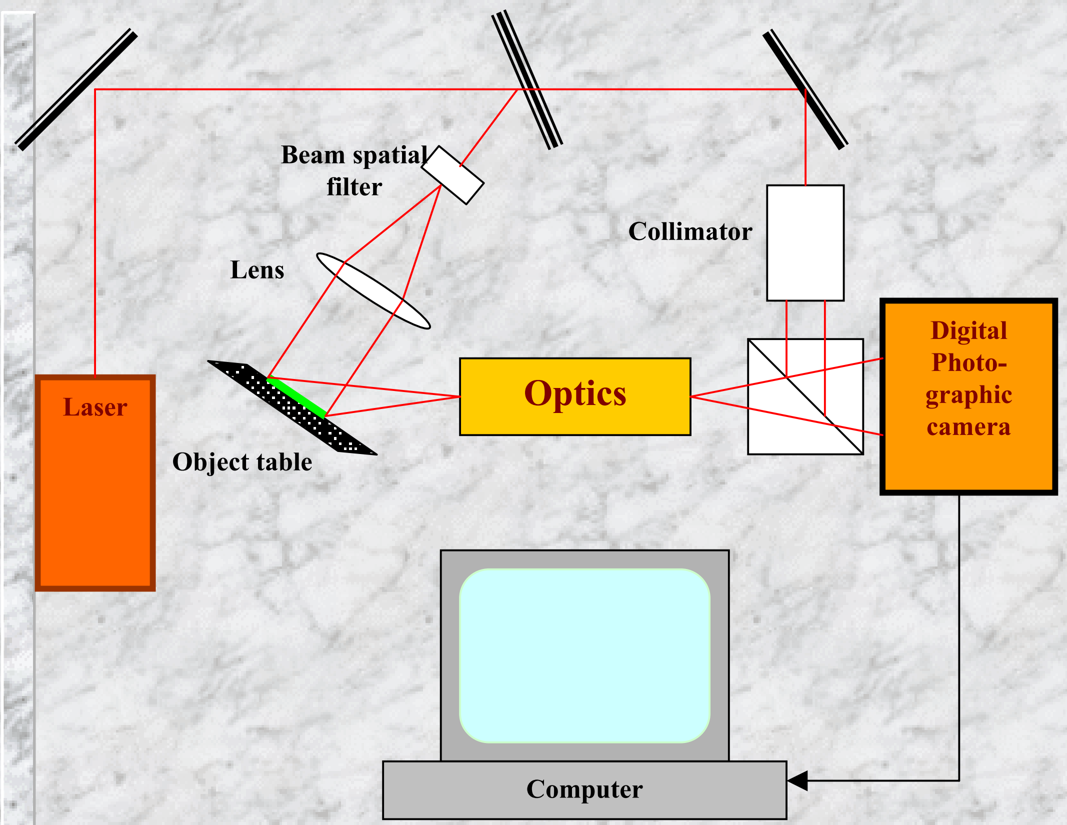

numerical reconstruction of electronically recorded optical holograms

Basic stages in numerical reconstruction of holograms

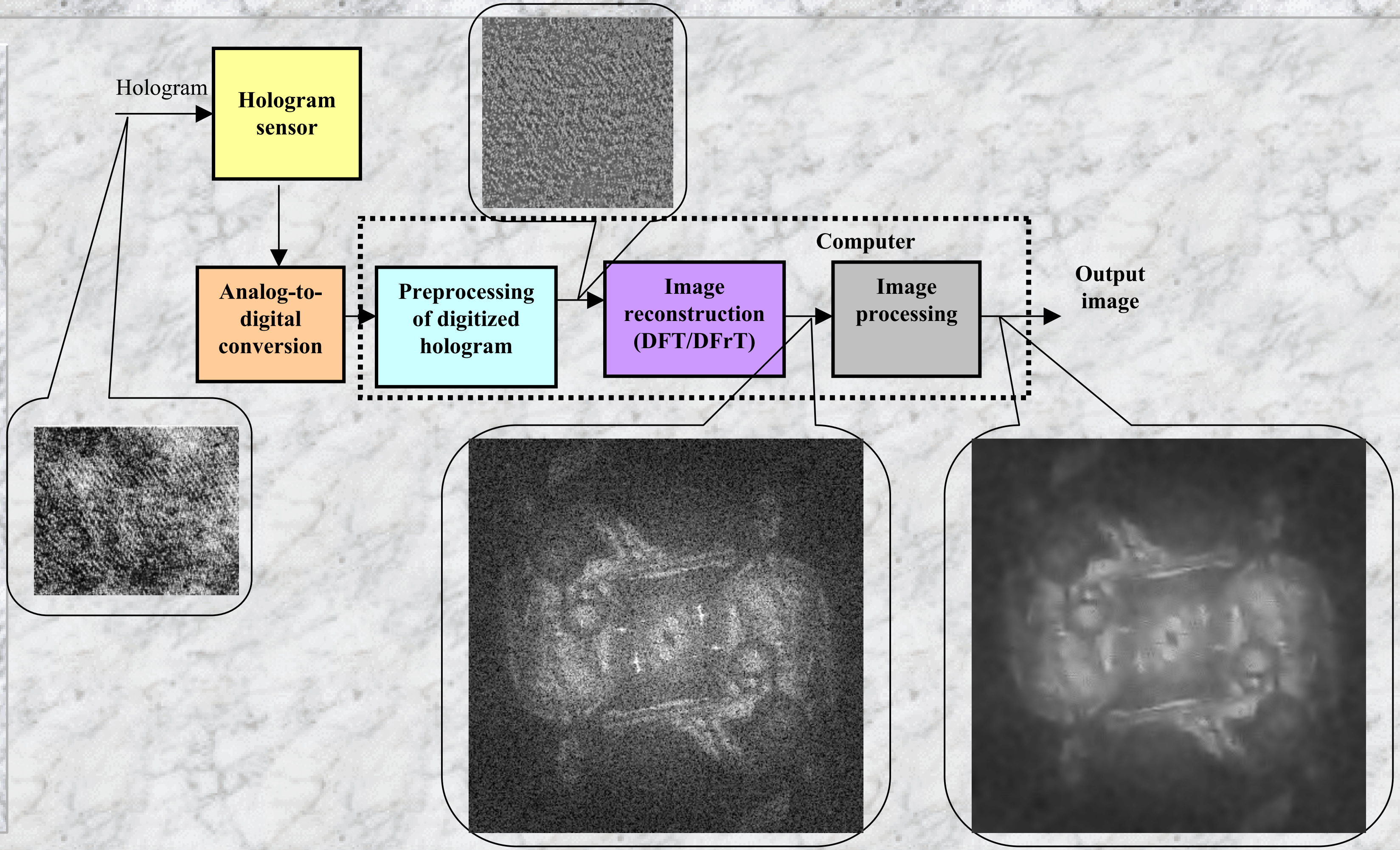

FAST TRANSFORMS FOR DIGITAL HOLOGRAPHY: Discrete Fourier transforms

Canonical Discrete Fourier Transform (DFT)	$\alpha_r = \frac{1}{\sqrt{N}} \sum_{k=0}^{N-1} a_k \exp\left(i2\pi \frac{kr}{N} \right)$
Shifted DFT	$\alpha_r^{u,v} = \frac{1}{\sqrt{N}} \sum_{k=0}^{N-1} a_k \exp\left[i2\pi \frac{(k+u)(r+v)}{N} \right]$
Discrete Cosine Transform (DCT)	$\alpha_r^{DCT} = \frac{2}{\sqrt{2N}} \sum_{k=0}^{N-1} a_k \cos\left(\pi \frac{k+1/2}{N} r \right)$
Discrete Cosine-Sine Transform (DcST)	$\alpha_r^{DcST} = \frac{1}{\sqrt{N}} \sum_{k=0}^{N-1} a_k \sin\left(\pi \frac{k+1/2}{N} r \right)$
Scaled DFT	$\alpha_r^{\sigma} = \frac{1}{\sqrt{\sigma N}} \sum_{k=0}^{N-1} a_k \exp\left[i2\pi \frac{(k+u)(r+v)}{\sigma N} \right] = \frac{1}{\sqrt{\sigma N}} \sum_{k=0}^{N-1} a_k \exp\left(i2\pi \frac{\tilde{k}\tilde{r}}{\sigma N} \right)$
Scaled DFT as a cyclic convolution	$\alpha_r^{\sigma} = \frac{\exp\left(i\pi \frac{\tilde{r}^2}{\sigma N} \right)}{\sqrt{\sigma N}} \sum_{k=0}^{N-1} \left[a_k \exp\left(i\pi \frac{\tilde{k}^2}{\sigma N} \right) \right] \exp\left[-i\pi \frac{(\tilde{k}-\tilde{r})^2}{\sigma N} \right]$
Canonical 2-D DFT	$\alpha_{r,s} = \frac{1}{\sqrt{N_1 N_2}} \sum_{k=0}^{N_1-1} \sum_{l=0}^{N_2-1} a_{k,l} \exp\left[i2\pi \left(\frac{kr}{N_1} + \frac{ls}{N_1} \right) \right]$
Affine DFT	$\alpha_{r,s} = \sum_{k=0}^{N_1-1} \sum_{l=0}^{N_2-1} a_{k,l} \exp\left[i2\pi \left(\frac{rk}{\sigma_A N_1} + \frac{sk}{\sigma_C N_1} + \frac{rl}{\sigma_B N_2} + \frac{sl}{\sigma_D N_2} \right) \right]$
Rotated Scaled DFT	$\alpha_{r,s} = \sum_{k=0}^{N-1} \sum_{l=0}^{N-1} a_{k,l} \exp\left[i2\pi \left(\frac{r\cos\theta - s\sin\theta}{\sigma N} k + \frac{r\sin\theta + s\cos\theta}{\sigma N} l \right) \right] =$
Discrete Sinc-function	$\mathrm{sincd}(N, x) = \frac{\sin x}{N \sin(x/N)}$

FAST TRANSFORMS FOR DIGITAL HOLOGRAPHY: Discrete Fresnel transforms

Canonical Discrete Fresnel Transform (DFrT)	$\alpha_r = \frac{1}{\sqrt{N}} \sum_{k=0}^{N-1} a_k \exp\left[i\pi \frac{(k/\mu - r\mu)^2}{N} \right] \qquad \mu^2 = \lambda Z / N \Delta f^2$
Shifted DFrT	$\alpha_r^{(\mu,w)} = \frac{1}{\sqrt{N}} \sum_{k=0}^{N-1} a_k \exp\left[-i\pi \frac{(k\mu - r/\mu + w)^2}{N} \right] \qquad w = u/\mu - v\mu$
Fourier Reconstruction algorithm for Fresnel holograms	$\alpha_r^{(\mu,w)} = \frac{\exp\left(-i\pi \frac{r^2}{\mu^2 N} \right)}{\sqrt{N}} \sum_{k=0}^{N-1} a_k \exp\left[-i\pi \frac{(k\mu + w)^2}{N} \right] \exp\left(i2\pi \frac{k + w/\mu}{N} r \right)$
Focal Plane invariant DFrT	$\alpha_r^{\left(\mu, \frac{N}{2\mu}\right)} = \frac{1}{\sqrt{N}} \sum_{k=0}^{N-1} a_k \exp\left\{ -i\pi \frac{[k\mu - (r - N/2)/\mu]^2}{N} \right\}$
Partial DFrT (PDFT)	$\tilde{\alpha}_r^{(\mu,w)} = \frac{1}{\sqrt{N}} \sum_{k=0}^{N-1} a_k \exp\left(-i\pi \frac{k^2\mu^2}{N} \right) \exp\left[i2\pi \frac{k(r - w\mu)}{N} \right]$
Focal plane invariant PDFrT	$\tilde{\tilde{\alpha}}_r^{(\mu,w)} = \frac{1}{\sqrt{N}} \sum_{k=0}^{N-1} a_k (-1)^k \exp\left(-i\pi \frac{k^2\mu^2}{N} \right) \exp\left(i2\pi \frac{kr}{N} \right)$
Convolutional Discrete Fresnel Transform (ConvDFrT)	$\alpha_r = \sum_{k=0}^{N-1} a_k \,\mathrm{frincd}(N; \mu^2; r + w - k) = \frac{1}{N} \sum_{s=0}^{N-1} \left[\sum_{k=0}^{N-1} a_k \exp\left(i2\pi \frac{k - r - w}{N} s \right) \right] \exp\left(-i\pi \frac{\mu^2 s^2}{N} \right)$
Convolutional reconstruction algorithm for Fresnel holograms	$\alpha_r = \frac{1}{N} \sum_{s=0}^{N-1} \left[\sum_{k=0}^{N-1} a_k \exp\left(i2\pi \frac{ks}{N} \right) \right] \exp\left(-i\pi \frac{\mu^2 s^2}{N} \right) \exp\left(-i2\pi \frac{r + w}{N} s \right)$
Frincd-function	$\mathrm{frincd}(N; q; x) = \frac{1}{N} \sum_{r=0}^{N-1} \exp\left(i\pi \frac{qr^2}{N} \right) \exp\left(-i2\pi \frac{xr}{N} \right)$

Reconstruction of a hologram on different distances using Fourier reconstruction algorithm (left), Fourier reconstruction algorithm with appropriate hologram masking to avoid aliasing (middle) and Convolution reconstruction algorithm

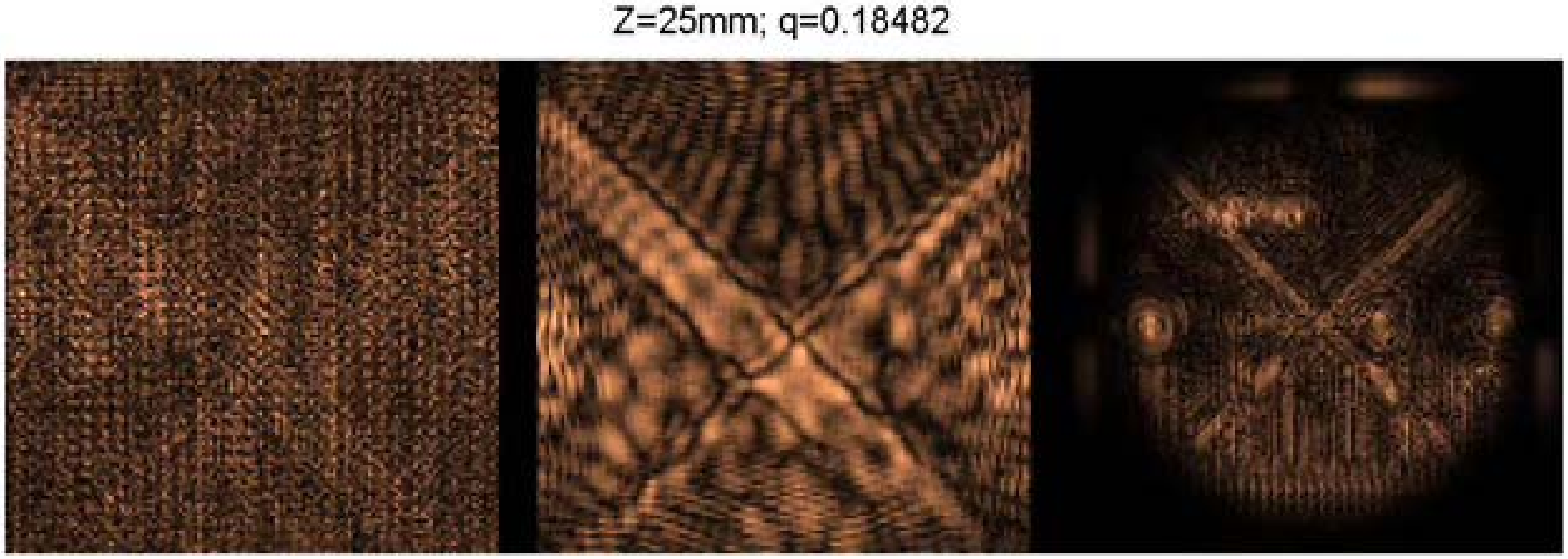

Hologram courtesy Dr. J. Campos, UAB, Barcelona, Spain

Hologram reconstruction: Fourier algorithm vs Convolution algorithm

Fourier reconstruction	Fourier reconstruction of the central part of the hologram free of aliasing	Convolution reconstruction

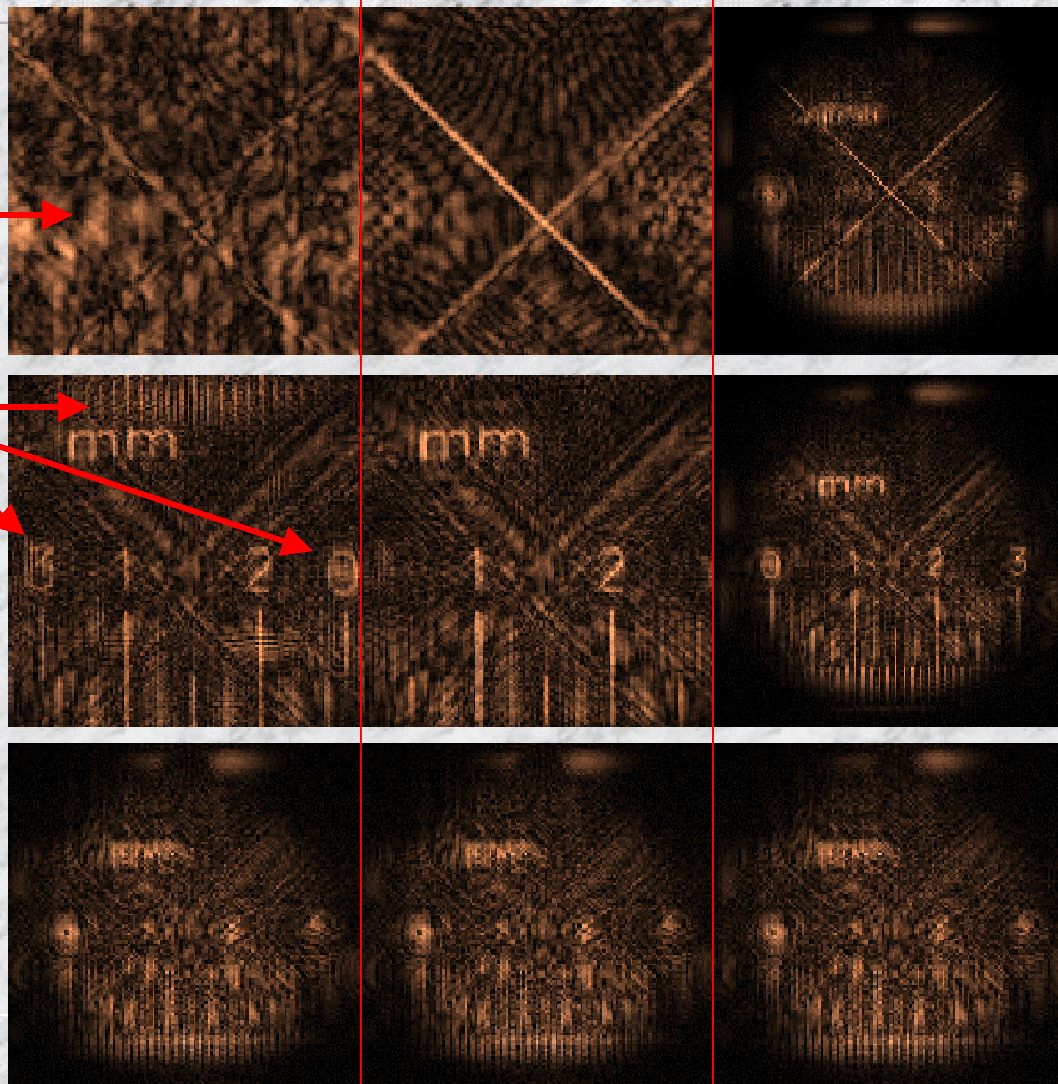

Image is destroyed due to the aliazing	Z=33mm; μ^2=0.2439
Aliasing artifacts	Z=83mm; μ^2 =0.6618
All restorations are identical	Z=136mm; μ^2 =1

Hologram courtesy Dr. J. Campos, UAB, Barcelona, Spain

Point spread function of numerical reconstruction of electronically recorded optical holograms

Digital reconstruction of samples of the object wave front amplitude from samples of its hologram is treated as a process of sampling the object wave front. Signal sampling is a linear transformation that is fully specified by its point spread function:

$$a_k = \int_X a(x) PSF(x,k)\, dx$$

Wave front samples

Object's wave front

Sampling device Point Spread Function

According to the sampling theorem, ideal sampling PSF is sinc-function

$$PSF(k,x) = \mathrm{sinc}[\pi(x - k\Delta x)/\Delta x]$$

$$= \frac{\sin[\pi(x - k\Delta x)/\Delta x]}{[\pi(x - k\Delta x)/\Delta x]}$$

Point Spread Functions of reconstruction of holograms recorded in far diffraction zone:

For hologram recording in far diffraction zone, wave propagation kernel $WP(x,f)$ is :

$$WP(x,f)=\exp(-i2\pi\frac{xf}{\lambda Z})$$

Assume that, for hologram reconstruction, shifted and scaled DFT is used with the reconstruction kernel:

$$DR(k,r)=\frac{1}{N}\exp\left[i2\pi\frac{k(r+v_T)}{\sigma N}\right]$$

where v_T and σ are shift and scale parameters

With this reconstruction kernel, point spread function of the reconstruction process $PSF^{FZ}(x,k)$ is

$$PSF^{FZ}(x,k)=\Phi^d(\frac{x}{\lambda Z})\exp\left\{-i2\pi\left[\frac{x}{\Delta x}\left(v_r+\frac{N-1}{2}\right)-\frac{k}{\sigma}\left(v_T+\frac{N-1}{2}\right)\right]\right\}\mathrm{sincd}\left[N,\pi\left(x-k\frac{\Delta x}{\sigma}\right)\Big/\Delta x\right]$$

where $\Phi^d(\frac{x}{\lambda Z})=\int_{-\infty}^{\infty}\varphi^d(f)\exp\left((-i2\pi\frac{xf}{\lambda Z})\right)df$ is frequency response of the hologram sampling device and

$$\Delta x=\lambda Z/S_H=\lambda Z/N\Delta f$$

$$\mathrm{sincd}(N,x)=\frac{\sin(x)}{N\sin(x/N)}$$

Define hologram discretization and reconstruction device coordinate system through the object coordinate system by choosing $v_r=v_T=(N-1)/2$. Then

$$PSF^{FZ}(x,k)=\Phi^d(\frac{x}{\lambda Z})\,\mathrm{sincd}\left[N_r,\pi\left(x-k\frac{\Delta x}{\sigma}\right)\Big/\Delta x\right]$$

PSF of reconstruction of holograms recorded in far diffraction zone (ctnd)

As one can see from the equation,

$$PSF^{FZ}(x,k) = \Phi^{d}\left(\frac{x}{\lambda Z}\right)\text{sincd}\left[N,\pi(x-k\Delta x)/\Delta x\right]$$

The point spread function is a periodical function of *k:*

$$PSF^{FZ}(k+g\sigma N_r) = (-1)^{g(N_r-1)} PSF^{FZ}(k);$$

(*g* is integer). It generates σN samples of object wavefront masked by the frequency response of the hologram recording and sampling device, the samples being taken with discretization interval

$$\Delta x/\sigma = \lambda Z/\sigma S_H = \lambda Z/\sigma N\Delta f$$

within the object size $S_o = \lambda Z/\Delta f$.

The case $\sigma = 1$ corresponds to a "cardinal" reconstructed object wavefront sampled with discretization interval $\Delta x = \lambda Z/S_H = \lambda Z/N\Delta f$. When $\sigma > 1$, reconstructed discrete wavefront is σ -times over-sampled, or σ -times zoomed-in. One can show that in this case the reconstructed object wavefront is a discrete sinc-interpolated version of the "cardinal" one.

PSF of reconstruction of holograms recorded in far diffraction zone (ctnd)

Discrete sinc-function is a discrete analog of the continuous sampling sinc-function, which is a point spread function of the ideal low-pass filter. As distinct from the sinc-function, discrete sinc-function is a periodical function with period $N\Delta x$ or $2N\Delta x$ depending on whether N is an odd or an even number and its Fourier spectrum is a sampled version of the frequency response of the ideal low pass filter

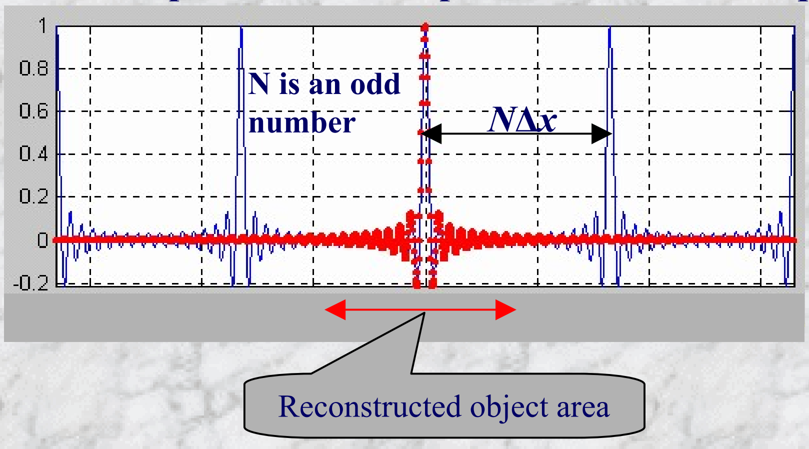

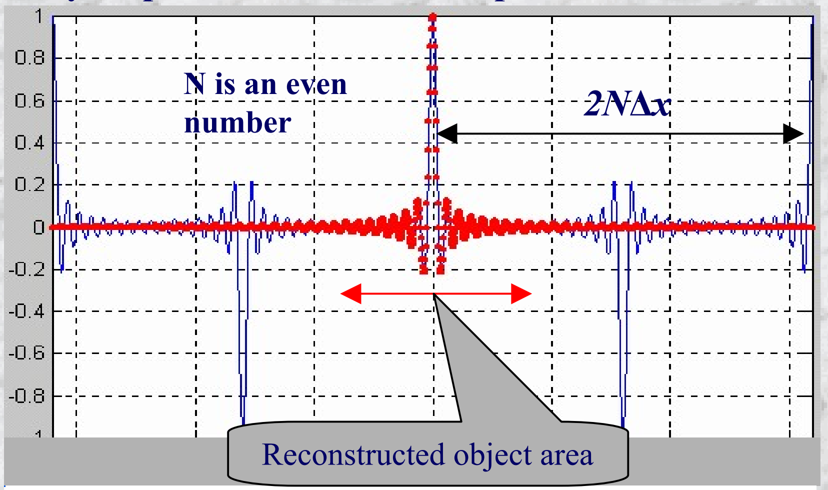

Continuous (red dots) and discrete (blue line) sinc-functions for odd and even number of samples *N*

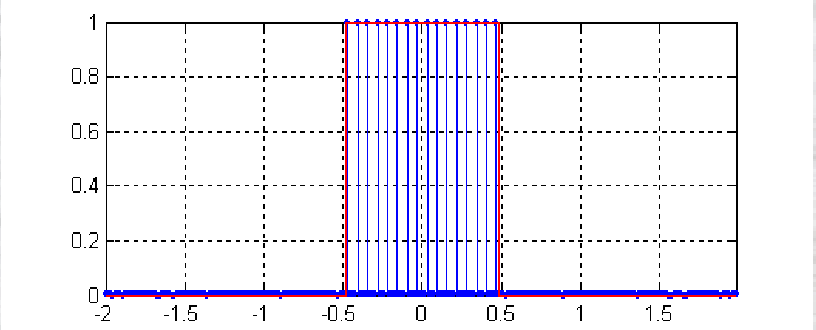

Frequency response of the ideal low pass filter (red) and Fourier transform of the discrete sinc-function (blue)

IMAGE PROCESSING

Target localization and tracking in cluttered multi-component images and video

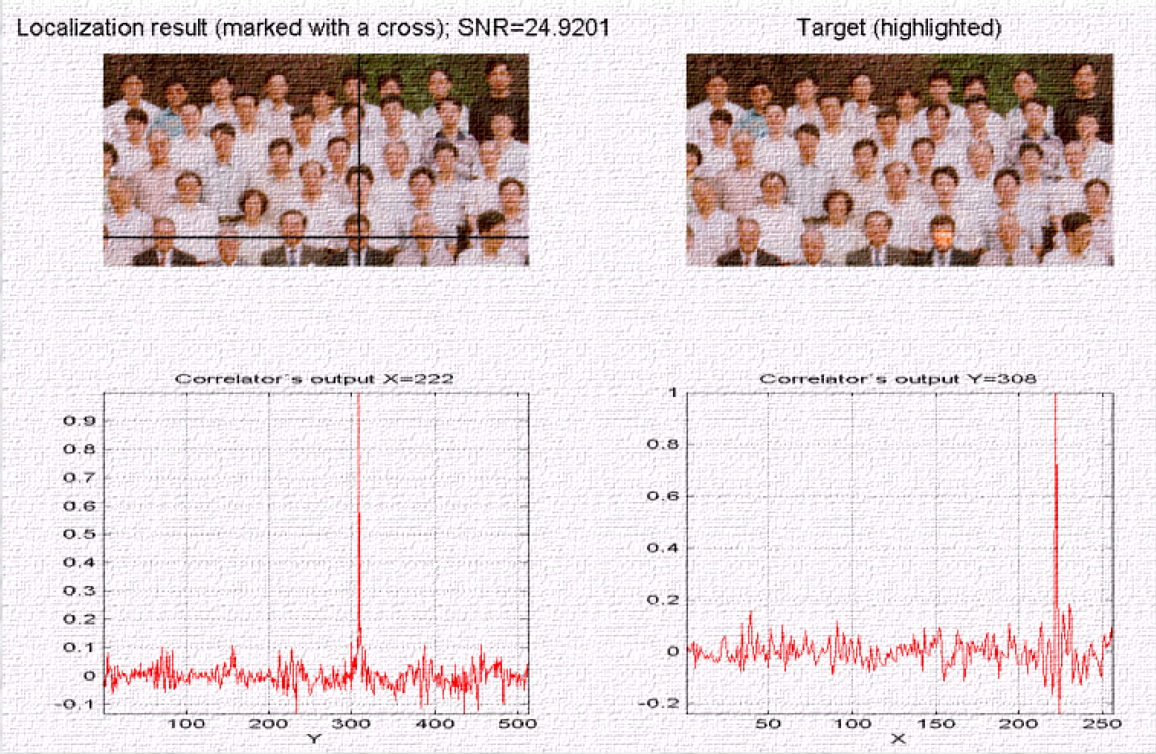

Object tracking in video sequencies: examples

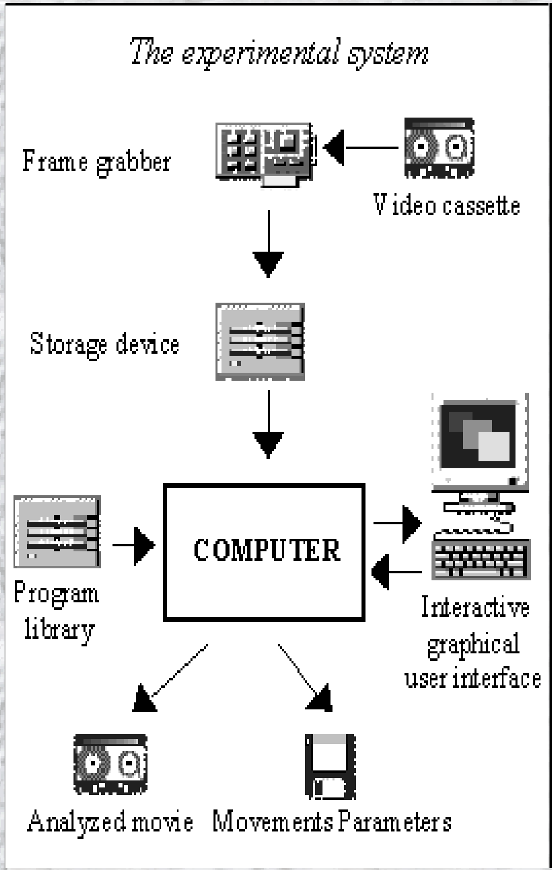

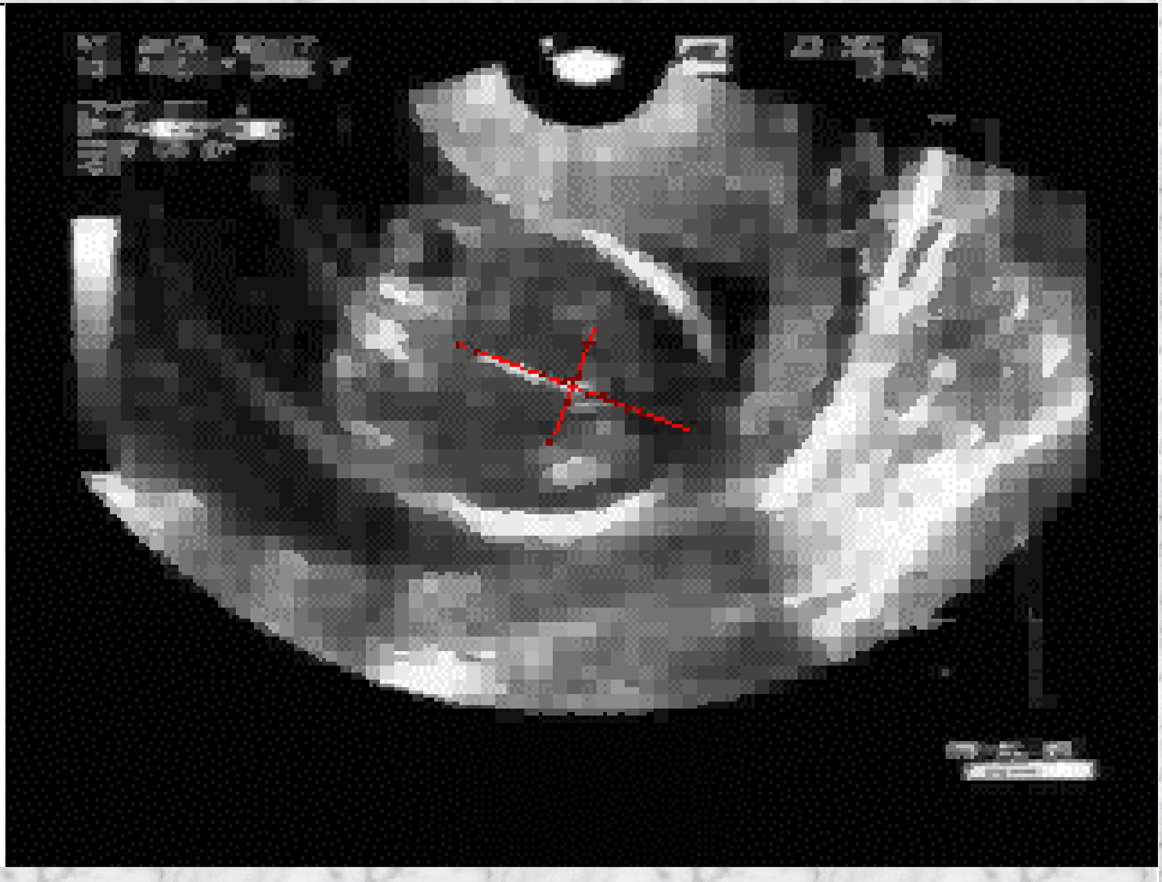

For details see http://www.eng.tau.ac.il/~yaro

Tracking fetus movements in Ultrasound movie

Face detection in complex images

The developed algorithm is capable of detecting, with high reliability, faces of varying size from minimum size of 12 pixels width and 15 pixels height to the maximum size of the input image.

The face detection capability of the developed system was experimentally examined on two test databases of images of high and low quality. The detection rates 96% and 84% were achieved for these databases, respectively.

http://www.eng.tau.ac.il/~yaro/Zion/ZionPhdSeminar4Web.pdf

Face detection: two-stage algorithm

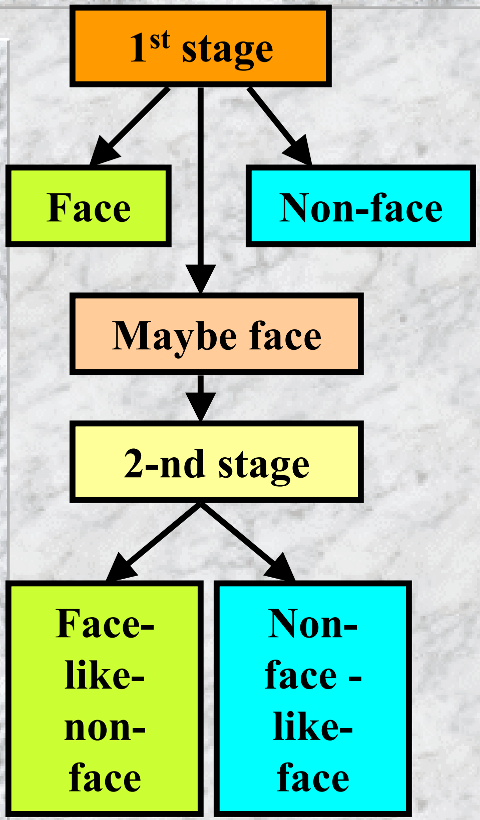

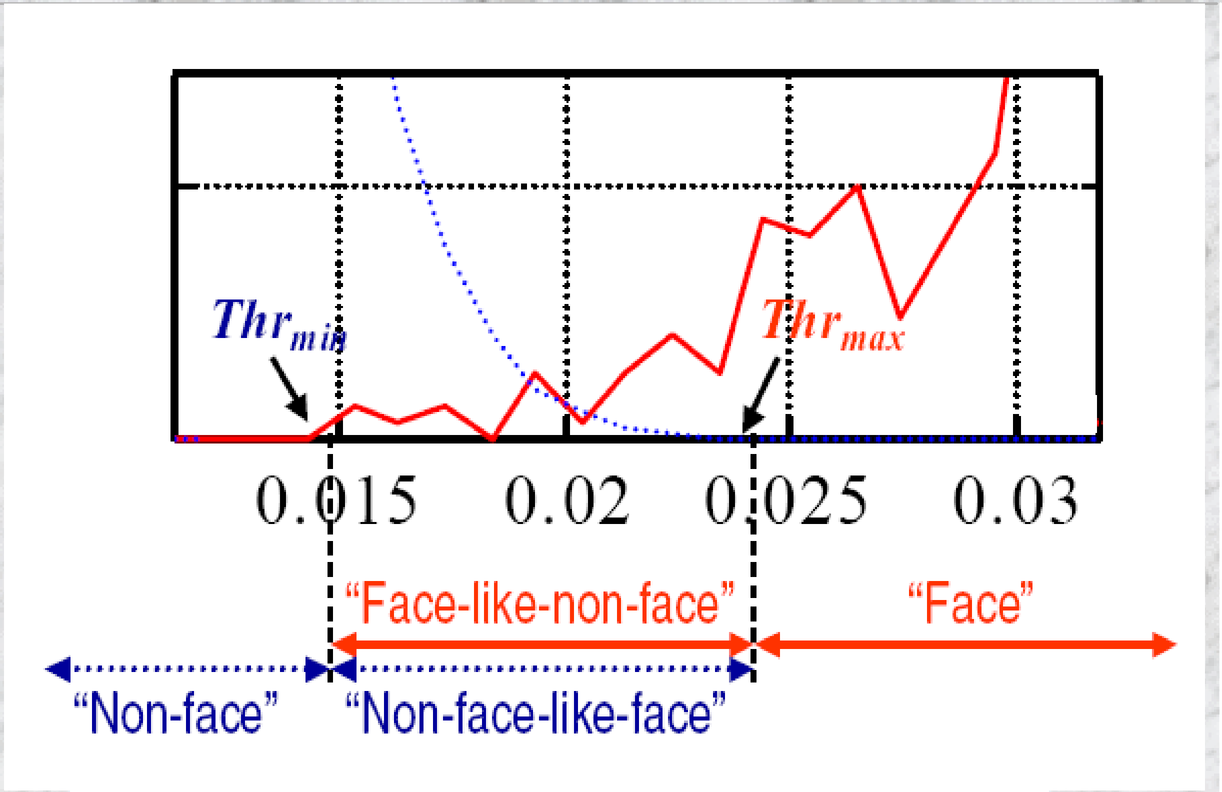

The "non-face" detection algorithm was proved to have "non-face" rejecting rate of ~99% and false alarm rate of 1.3% (faces wrongly rejected), thus leaving only 1% of the image area for subsequent thorough analysis by the "multi-template classification" algorithm. The algorithm is fast and requires approximately 200 flops per pixel in an input image of 640480 pixels size.

Face detection: Face-like-non-face and non-face-like face data bases

"Multi-template classification" algorithms use a very large set of templates prepared for different target shapes and varying illumination conditions. The developed algorithms were trained using a specially created training database obtained by extending four "face" databases to 32,000 images and one "non-face" database to one million images by means of scaling and rotating database images. In particular, "face", "non-face", "faces like clutter" and "clutter like faces" templates were generated from these training databases.

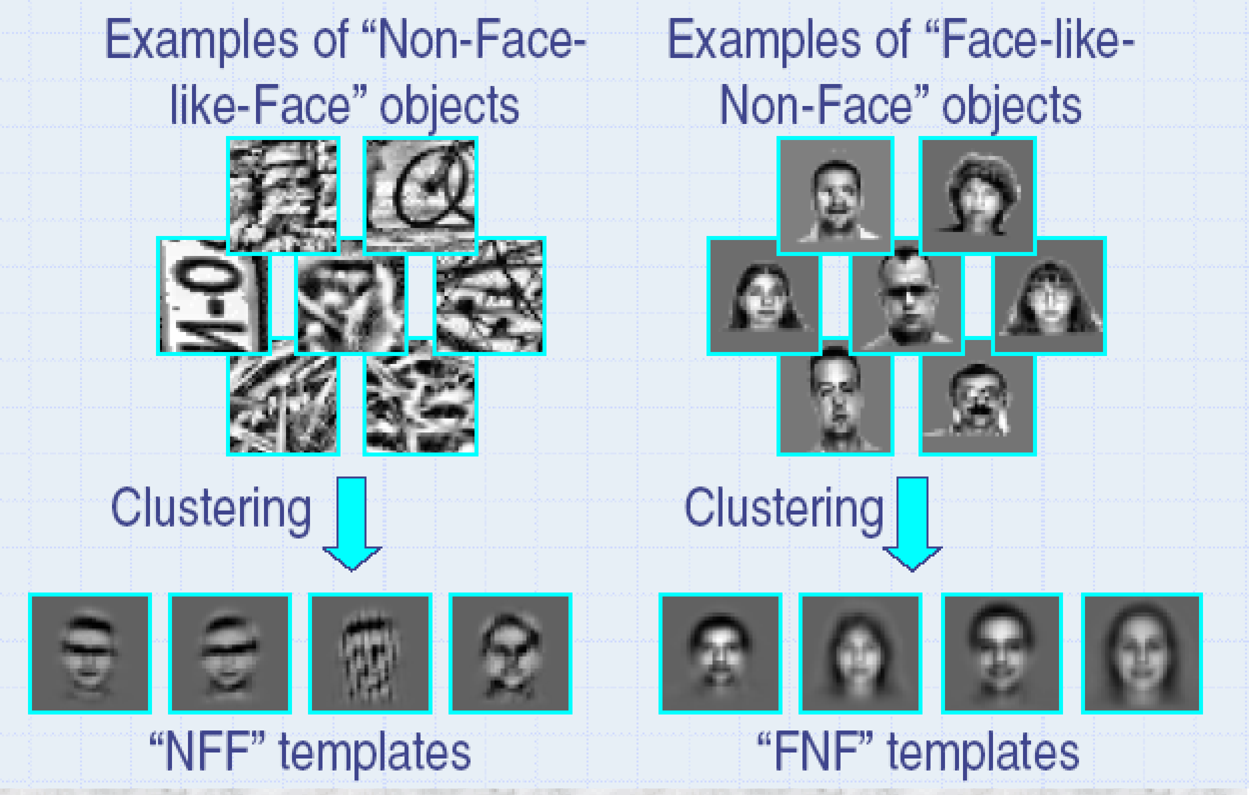

IMAGE PROCESSING

MULTI COMPONENT IMAGE RESTORATION:
Spatial/temporal adaptive linear filters

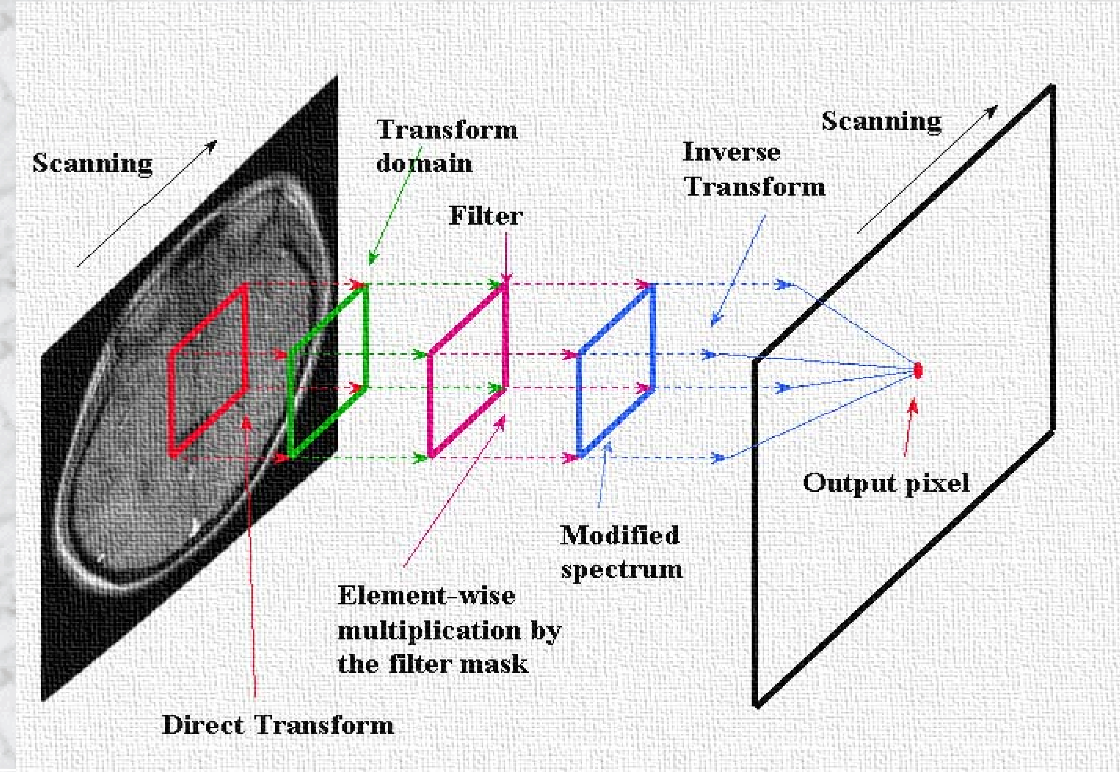

Color image de-noising and deblurring

3-D Local adaptive spatial-temporal filtering: denoising and deblurring of thermal video

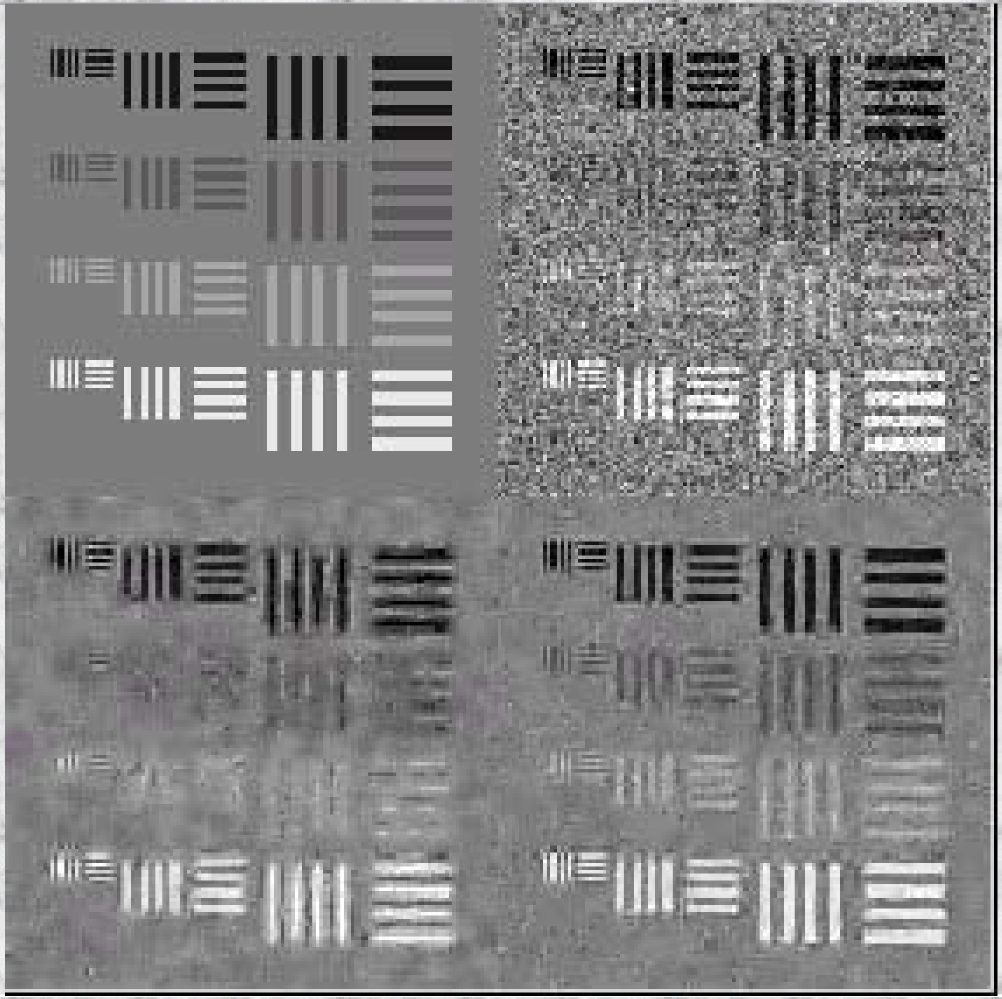

3-D Local adaptive spatial-temporal filtering: denoising and deblurring of thermal video (ctnd)

Before **After**
(5x5x5 DCT domain filtering)

Stabilization and restoration of atmospheric turbulent video

Restored stabilized video with moving objects unaffected	Moving objects	Initial video
	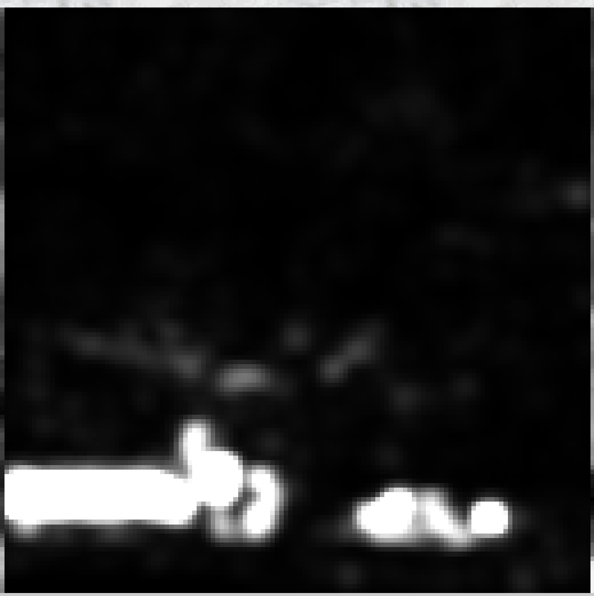	

Turbulent atmosphere video

Stabilized turbulent atmosphere video

IMAGE PROCESSING:

Fast interpolation error free discrete sinc-interpolation algorithms for image resampling and geometrical transformations:

Boundary effect free discrete sinc-interpolation in DCT domain

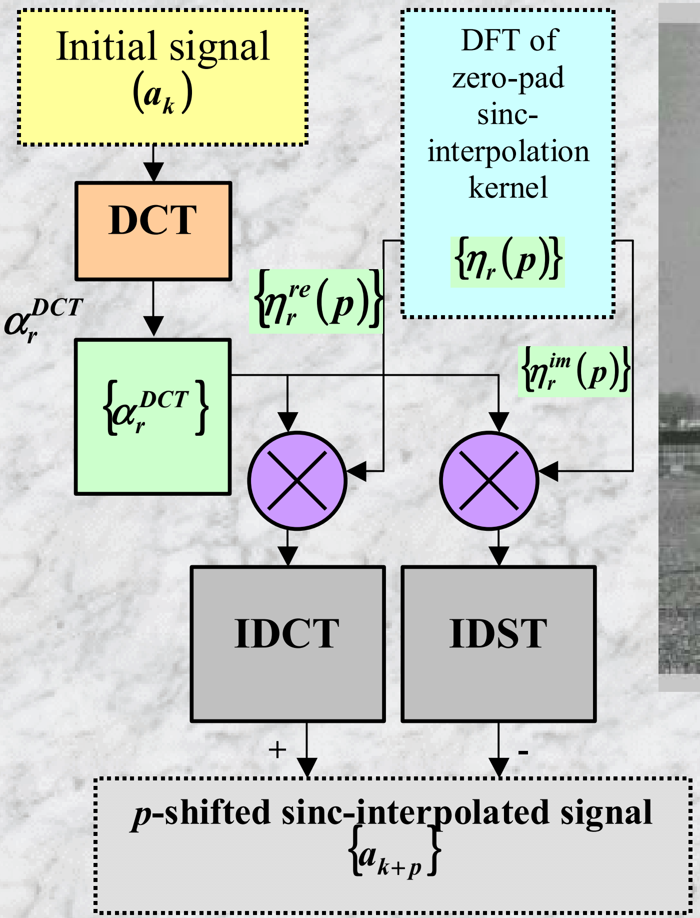

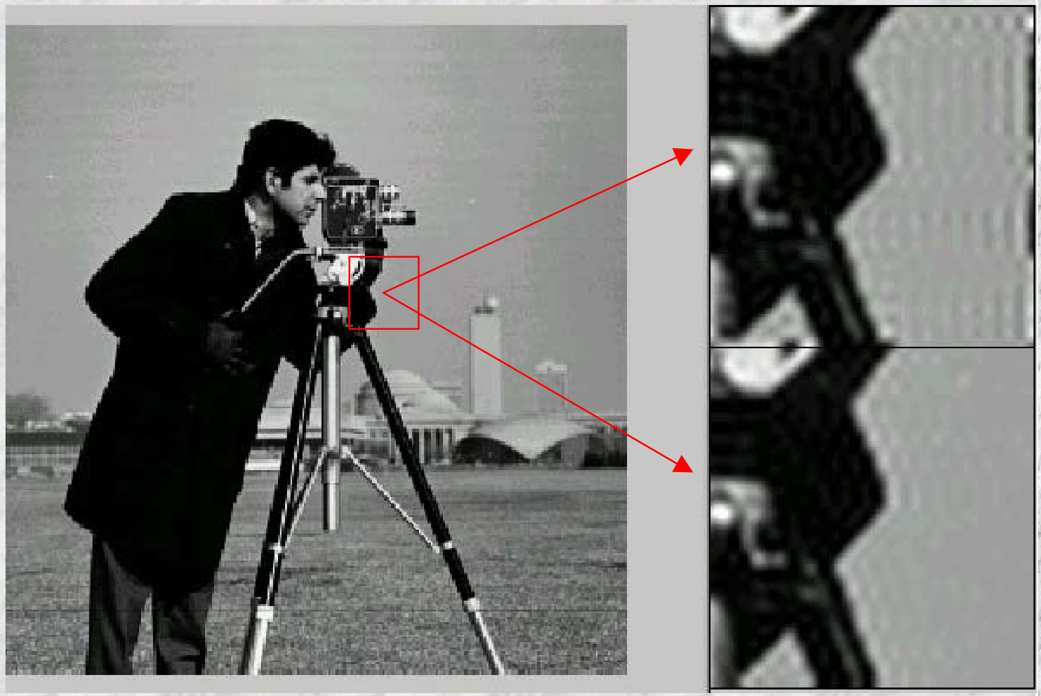

Zooming an image fragment (left) by sinc-interpolation in DFT domain (right upper image) and in DCT domain (right bottom image). Oscillations due to boundary effects that are clearly seen in DFT-interpolated image completely disappear in DCT-interpolated image.

Comparison of interpolation distortions:

higher order spline interpolator vs discrete sinc-interpolator

18,000º - rotated images in 1000 steps

High order Spline531:

~0.7 sec/rotation

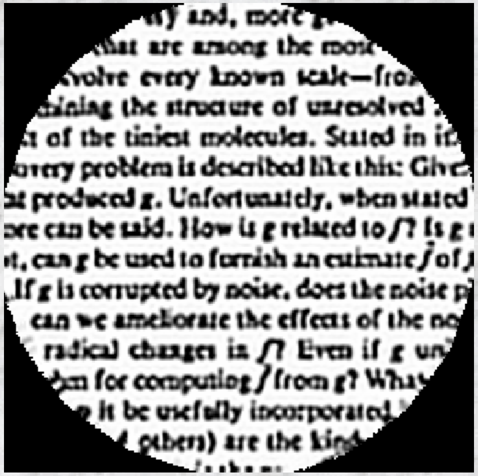

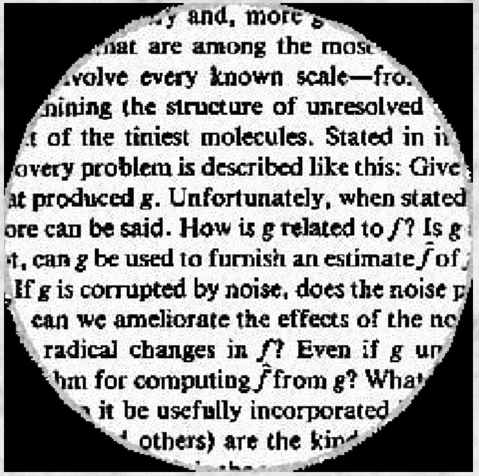

DFTsinc

~0.7 sec/rotation

Image low pass filtered to 0.5 of the base band

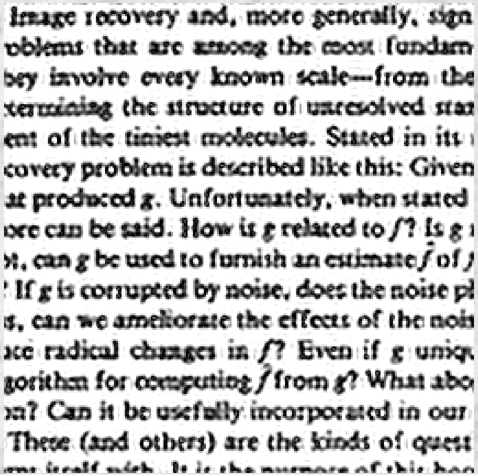

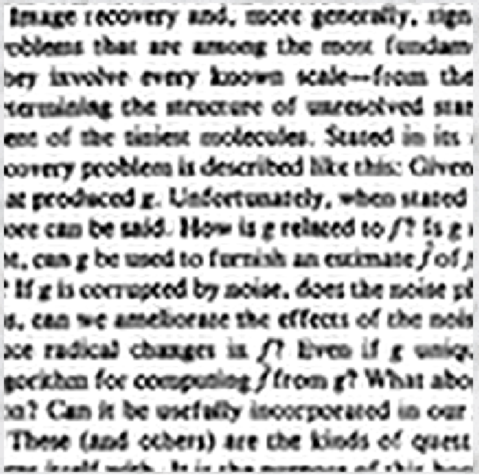

Image low pass filtered to 0.4 of the base band

Spline interpolation and discrete sinc-interpolation:

Rotation error spectra: 10 rotations through 36^o

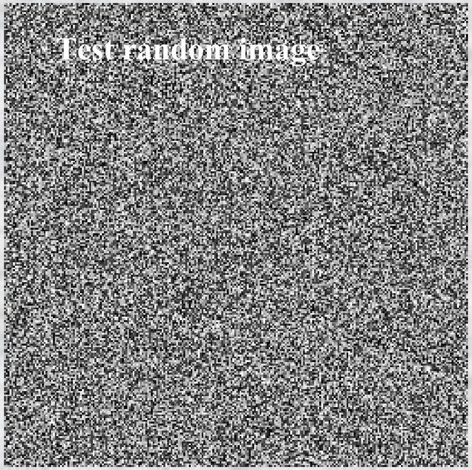

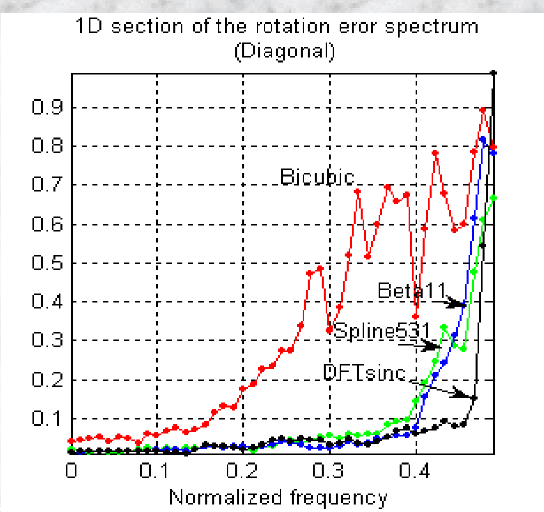

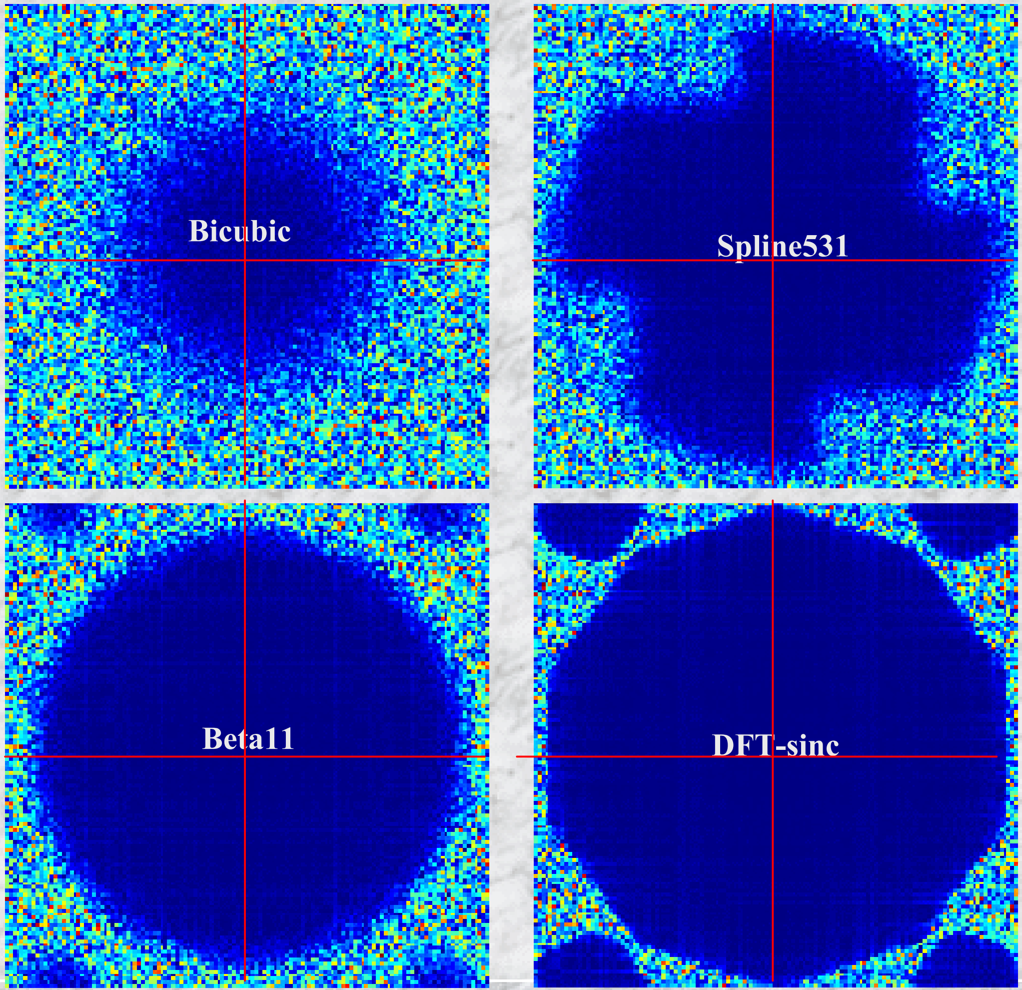

Comparison of interpolation accuracy of different interpolation techniques:

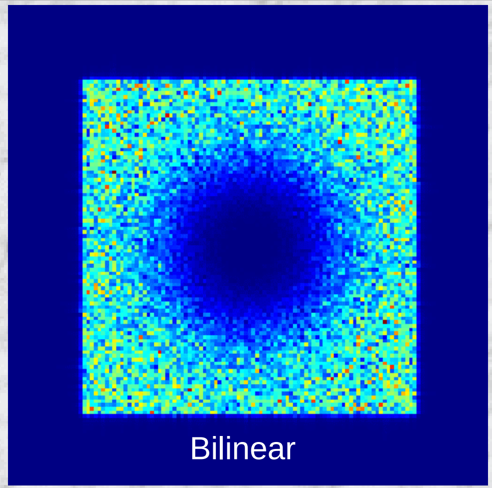

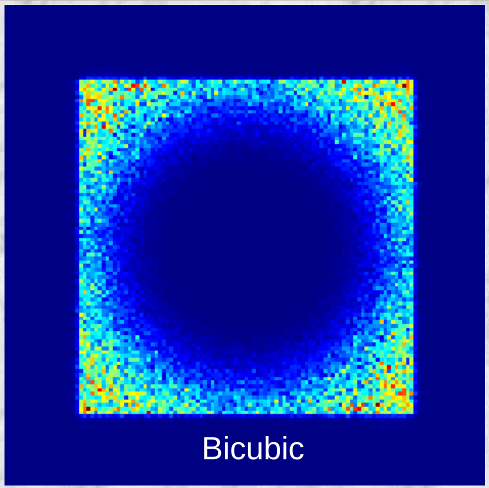

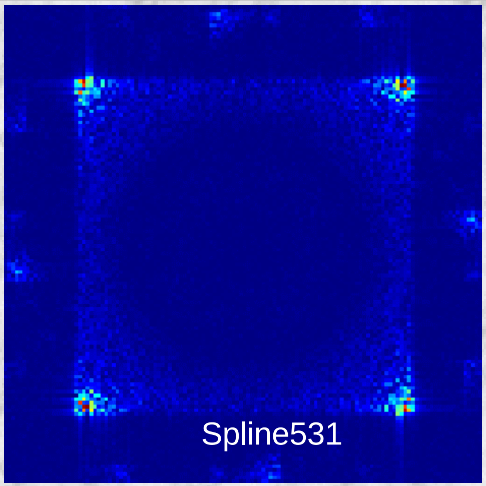

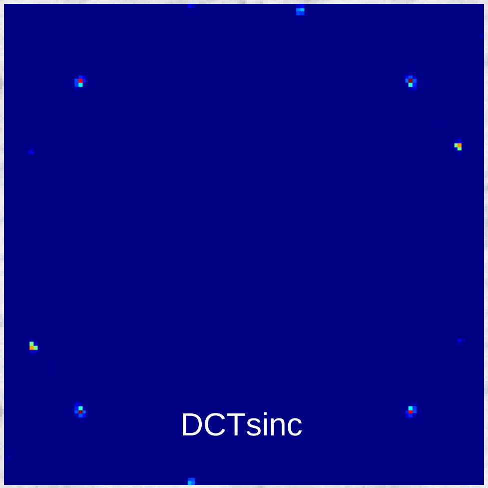

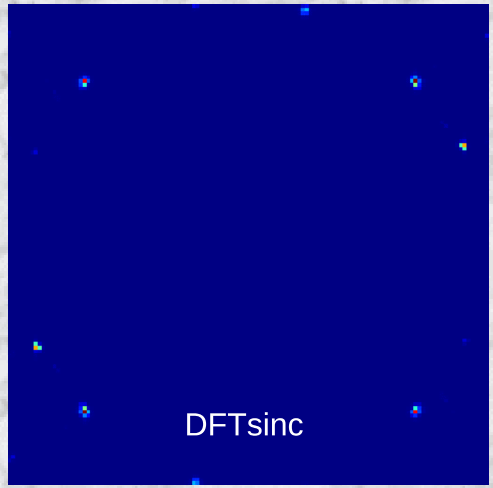

Spectra, for $10X36^{o}$ rotations, of the test random image low pass filtered to 0.7 of the base band

Discrete-sinc-interpolated image resizing using Scaled DFT

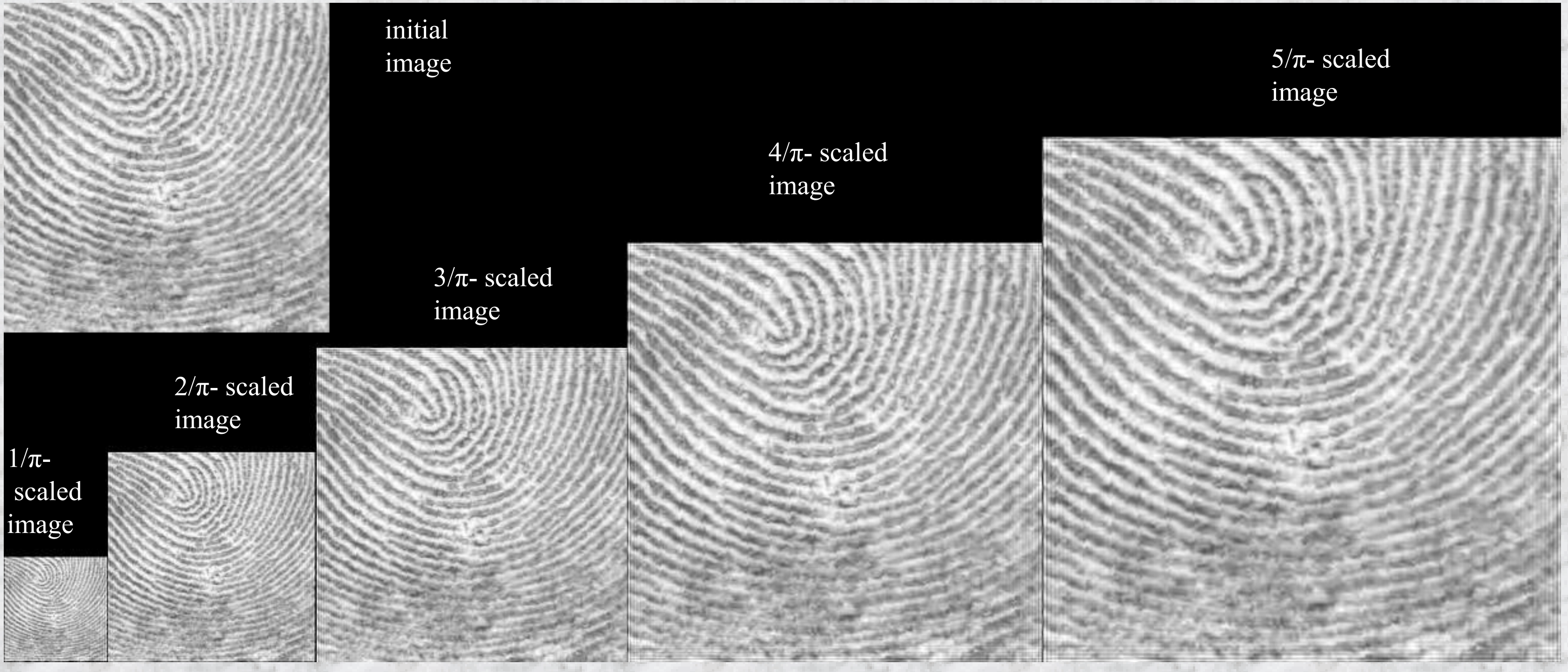

Using RotDFT-based rotation/resizing algorithm for simultaneous image rotation, resizing and enhancement

Initial image

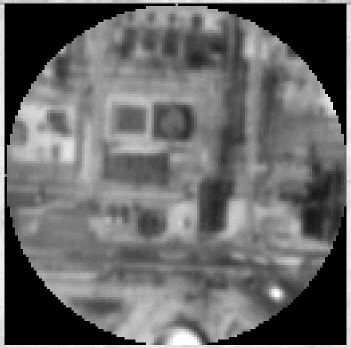

10^o-rotated and 1.7X-magnified image

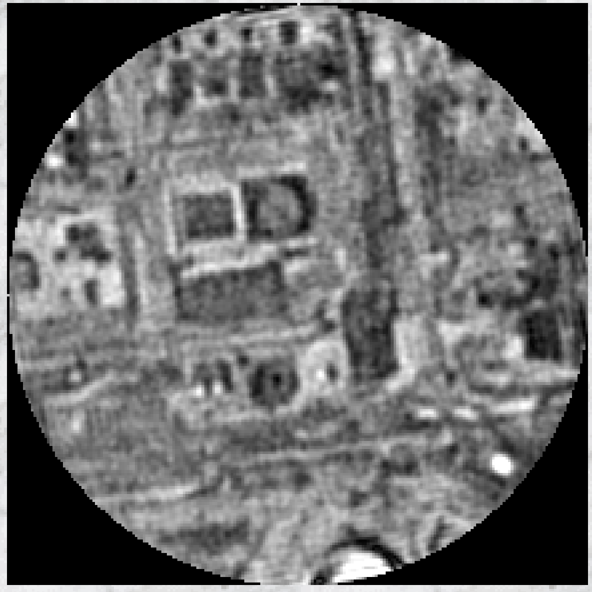

10^o-rotated, 1.7X-magnified and *P*-th law spectrum compression enhanced (*P*=0.5) image

tul128orig_0noise

;tul_0rand_x17%10_P10%10Th0%10.tif

tul_0rand_x17%10_P5%10Th25%10.tif

Image arbitrary mapping in sliding window

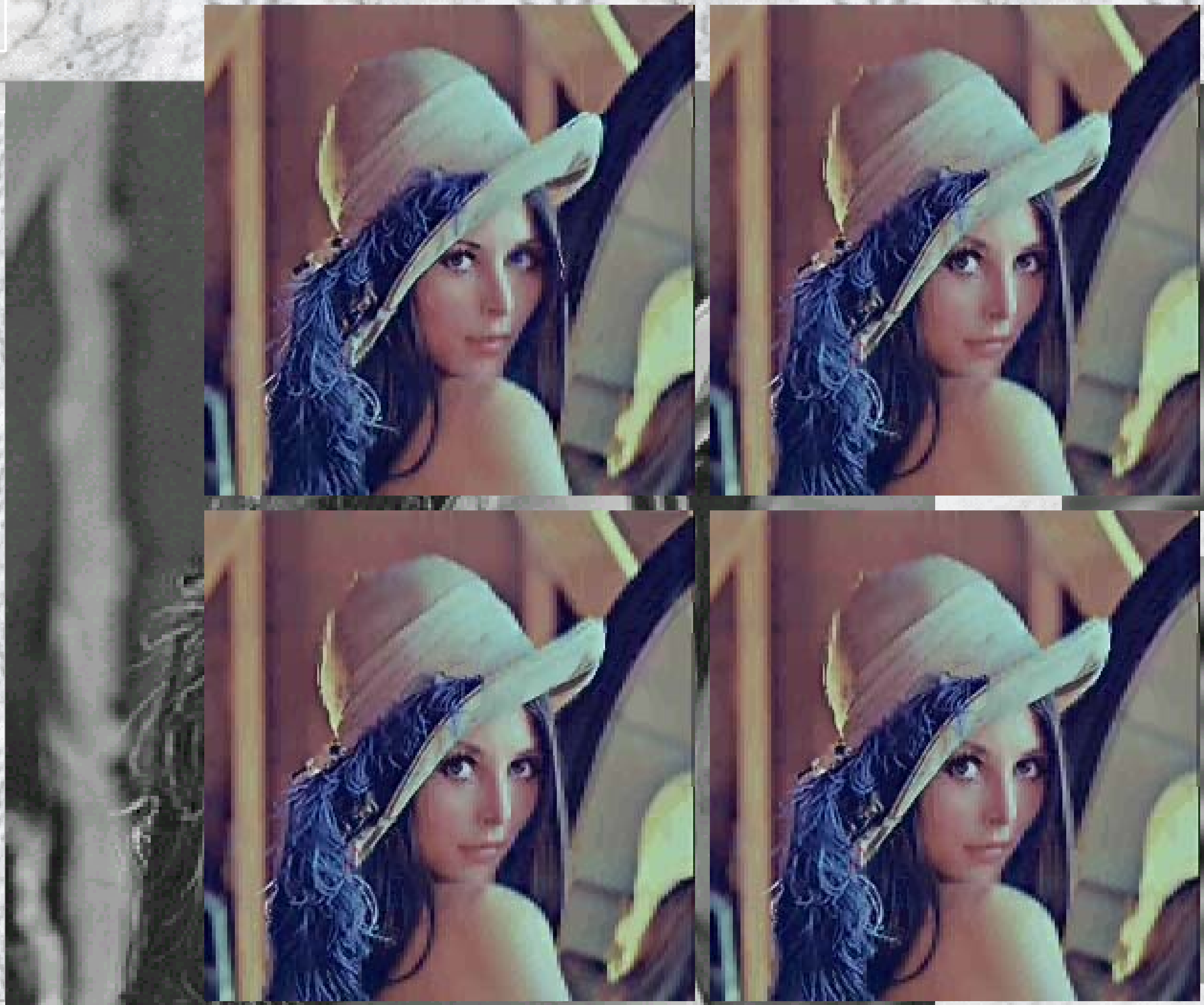

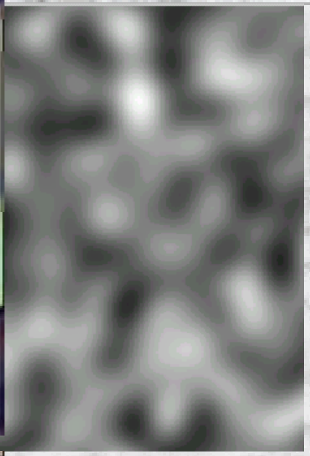

MapX

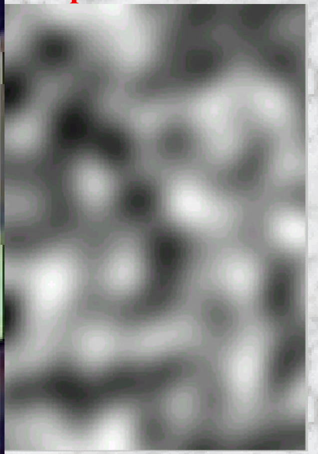

MapY

lcmapping_arbitr(len,(mapX+i*mapY)/1.5,8,8)

Sliding window discrete sinc-interpolation in DCT domain:

Simultaneous image resampling and restoration/enhancement

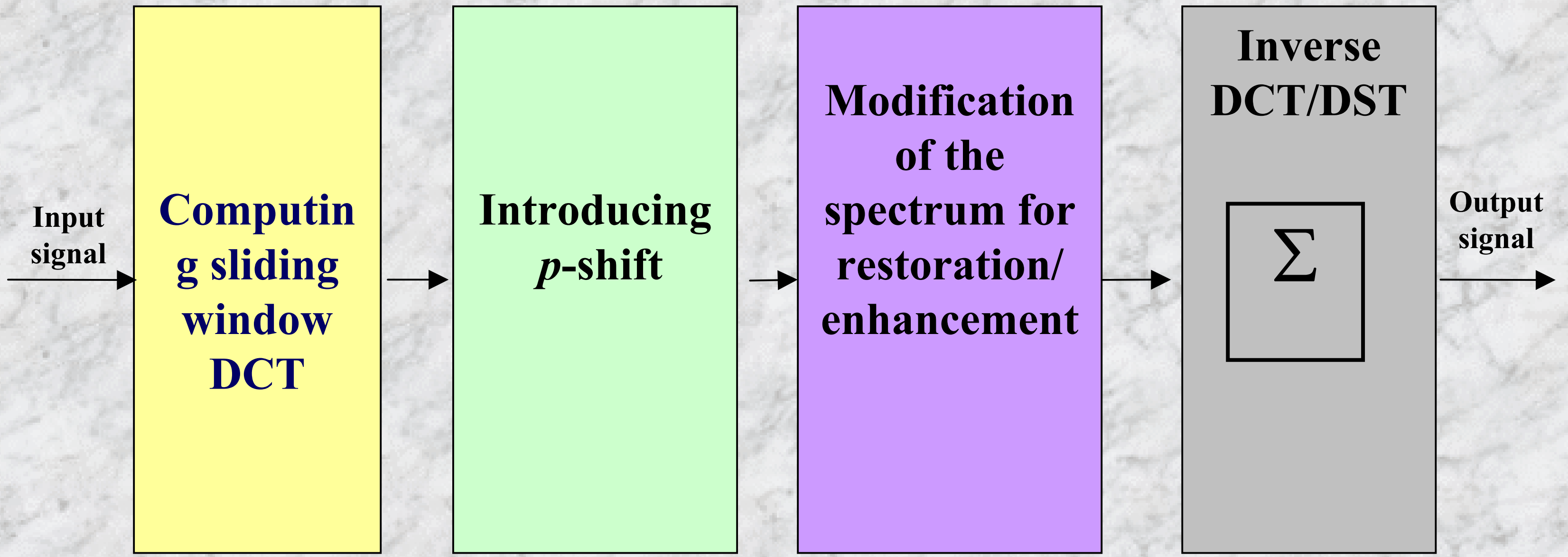

Sliding window sinc-interpolation in DCT domain: signal resampling and denoising

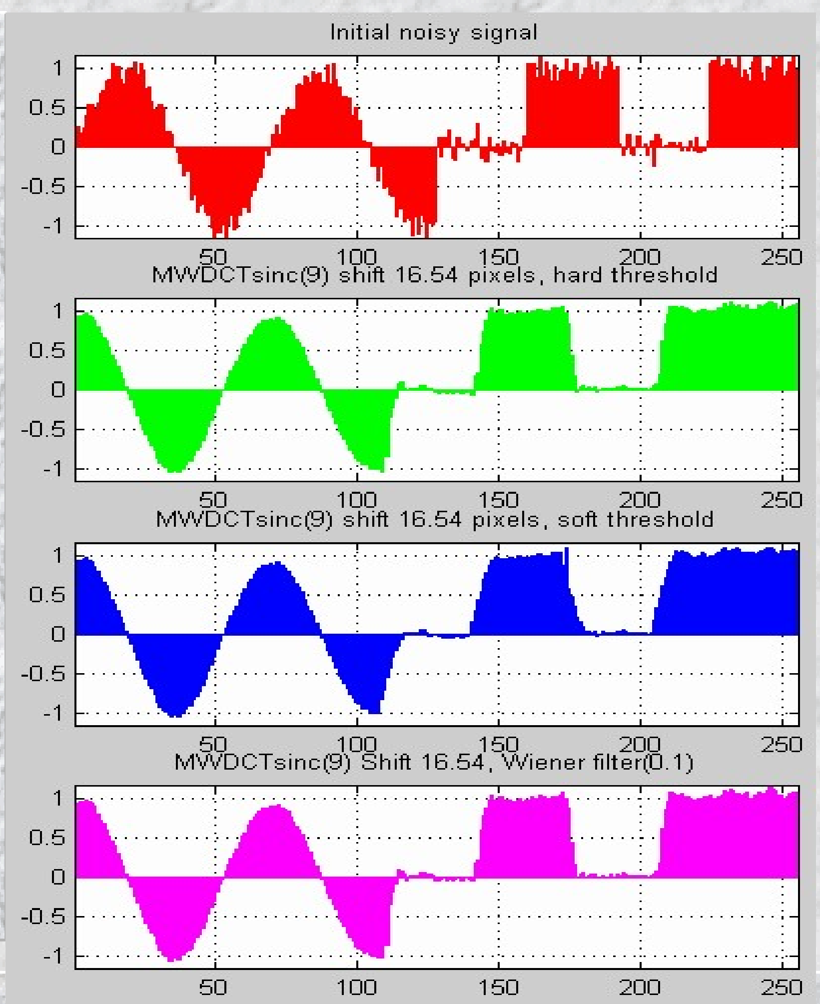

Noisy image (a) and a result of the rotation and denoising with sliding window DCT sinc-interpolation and denoising (b).

Sliding window sinc-interpolation DCT domain: local adaptive interpolation

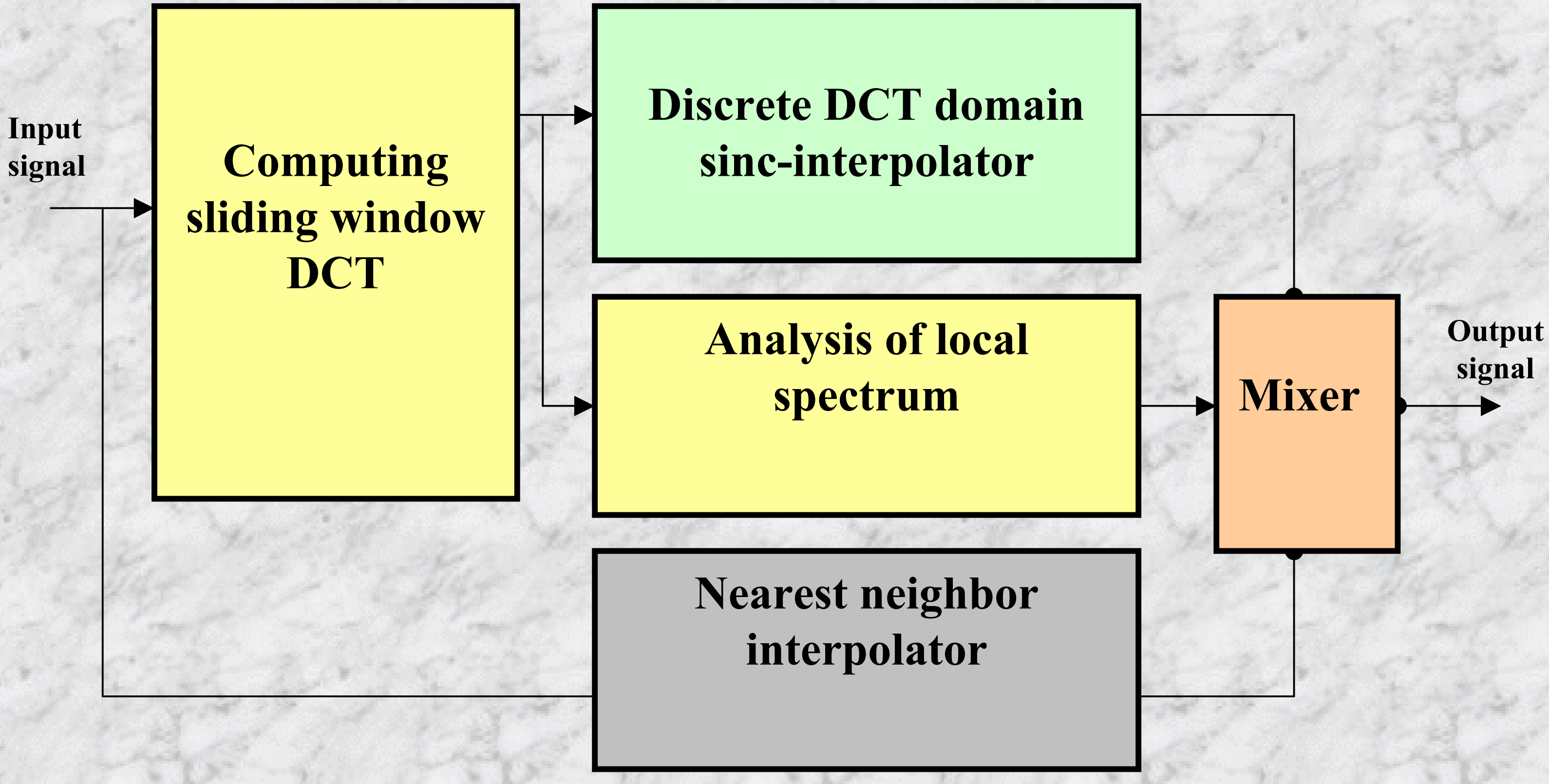

Adaptive versus non adaptive signal interpolation

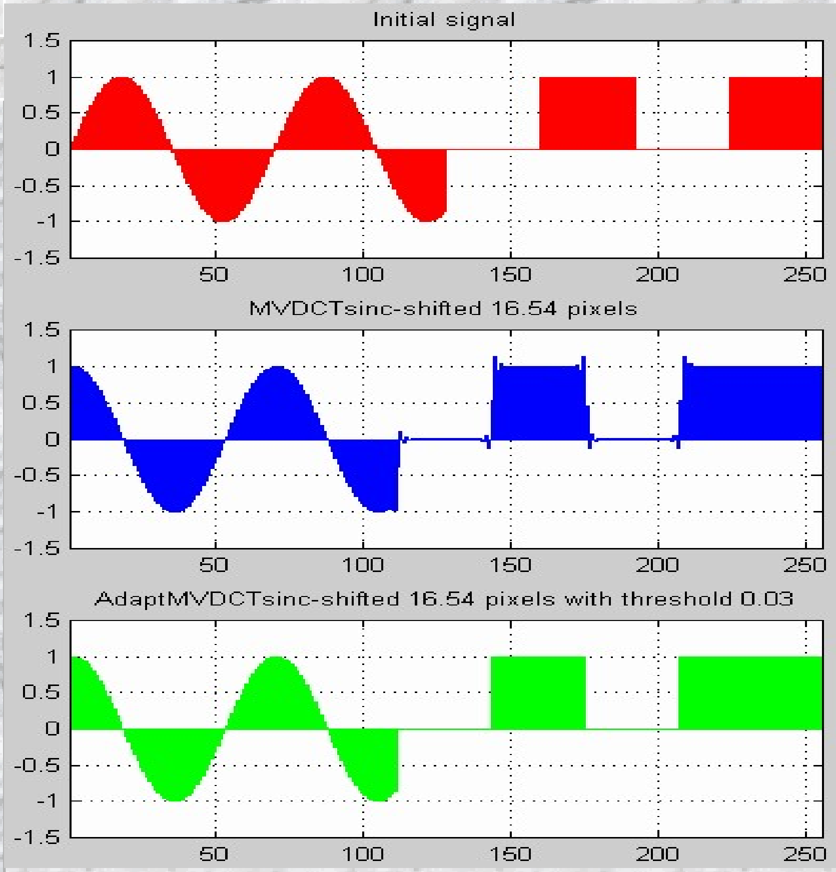

Signal (upper plot) shift by non-adaptive (middle plot) and adaptive (bottom plot) sliding window DCT sinc-interpolation. One can notice disappearance of oscillations at the edges of rectangle impulses when interpolation is adaptive.

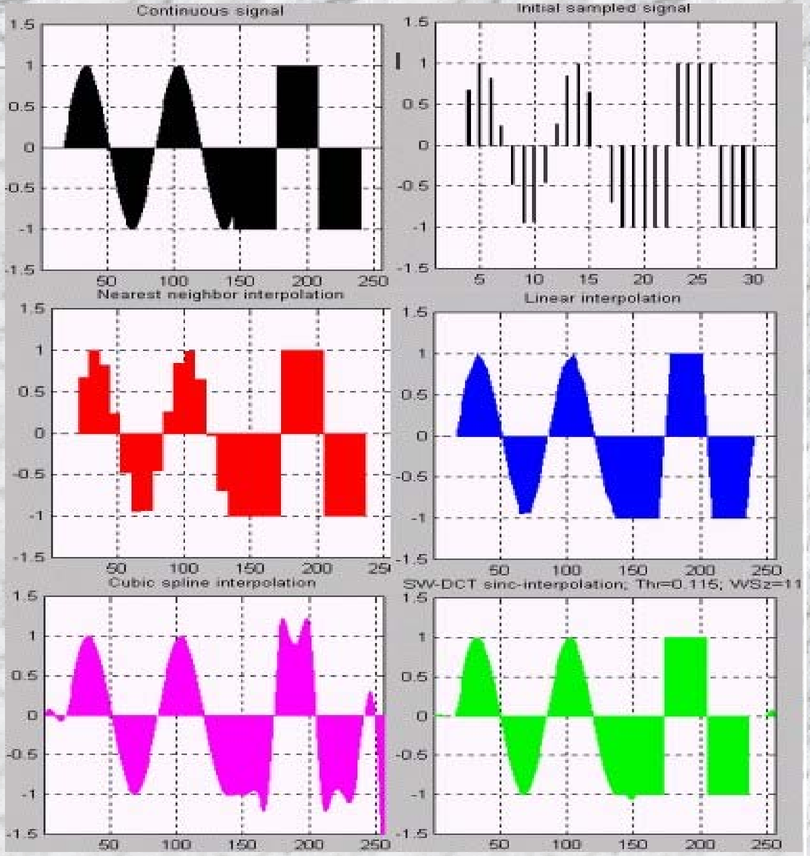

Comparison of nearest neighbor, linear, bicubic spline and adaptive sliding window sinc interpolation methods for zooming a digital signal (From left to right, from top to bottom: Continuous signal; initial sampled signal; nearest neighbor -interpolated signal ; linearly -interpolated signal; cubic spline -interpolated signal; sliding window sinc-interpolated signal).

Image rotation with adaptive and non-adaptive discrete sinc interpolation

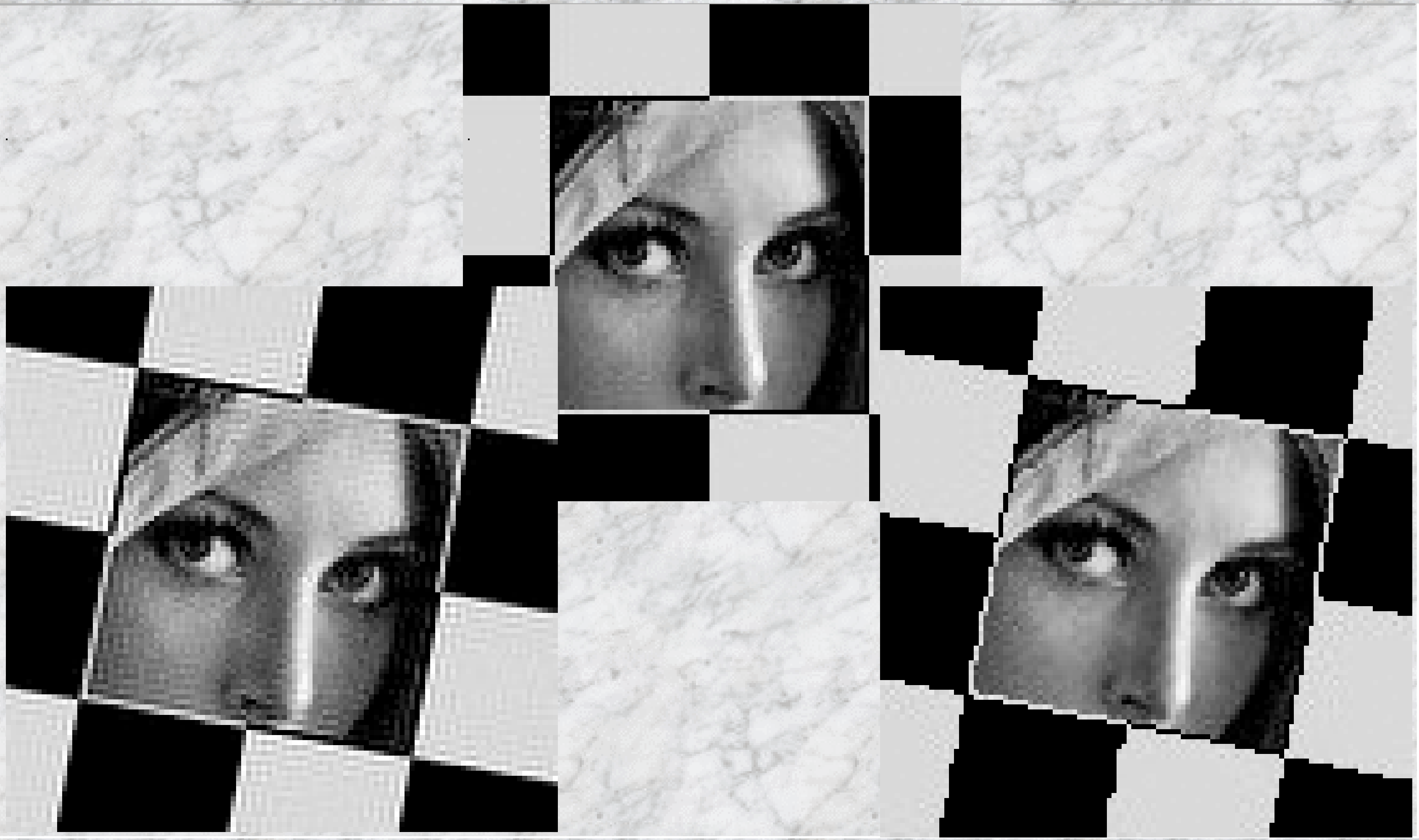

IMAGE PROCESSING

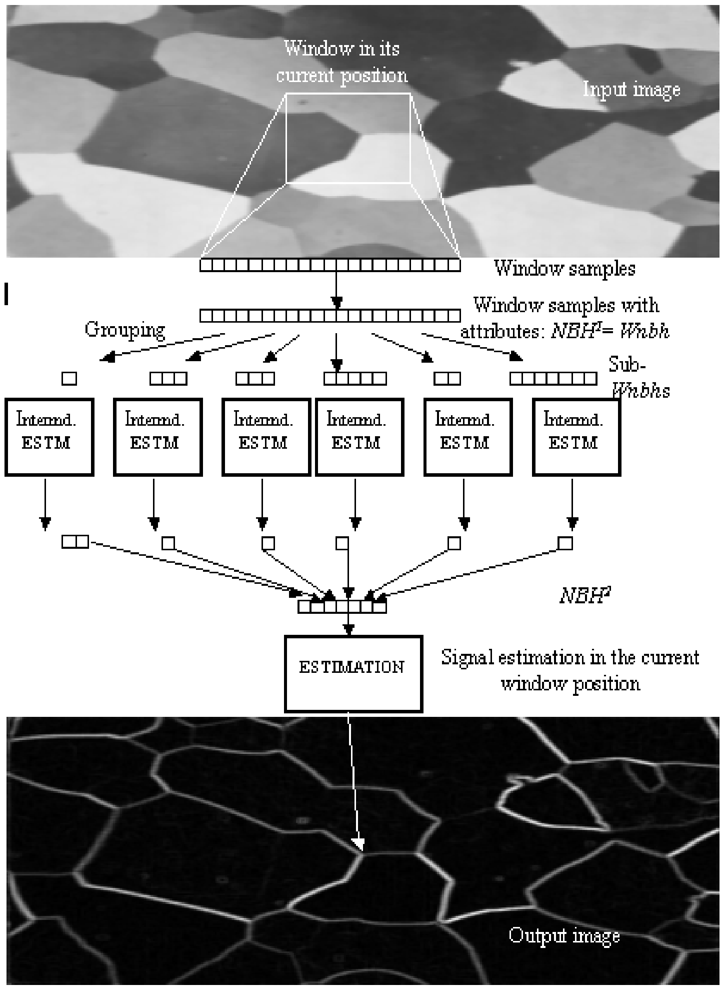

Nonlinear (rank) filters for image de-noising and enhancement

Rank filters for image de-noising and enhancement

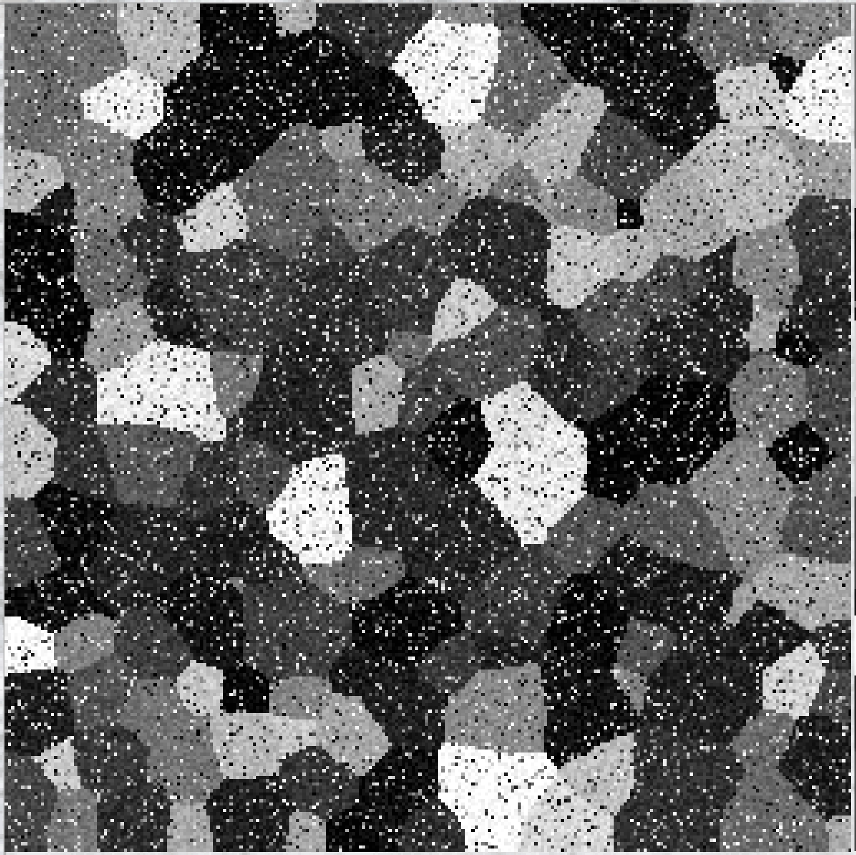

Noisy image, stdev = 20, Pn=0.15

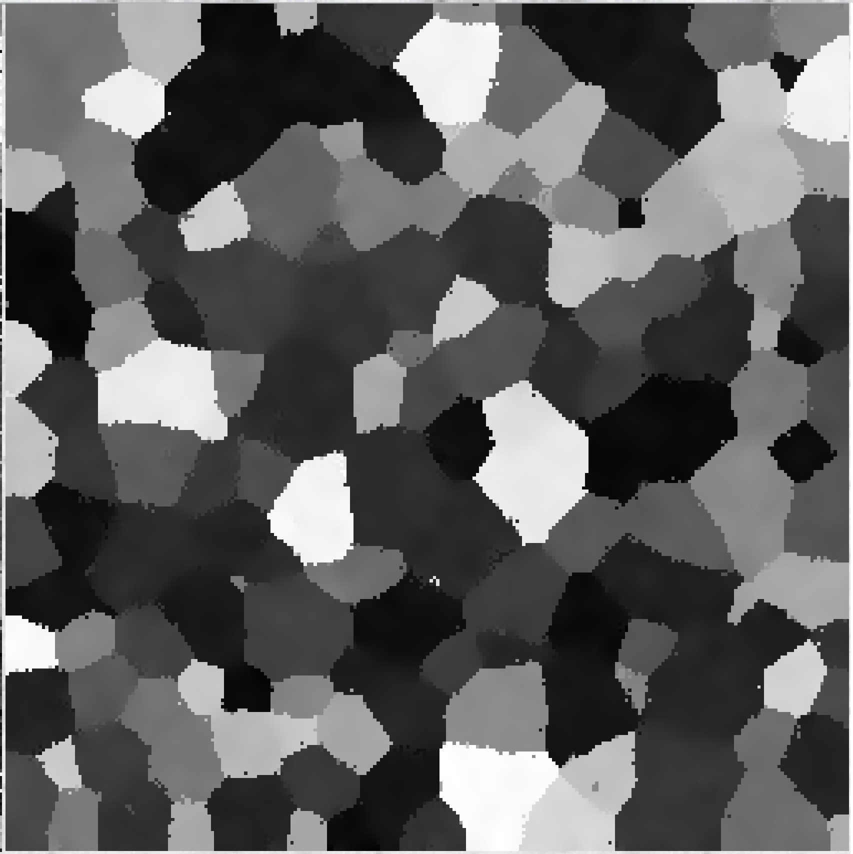

Iterative SCSigma-filter .
Window 5x5, Evpl=Evmn=15; 5 iterations

Nonlinear filters: Image enhancement

Initial image

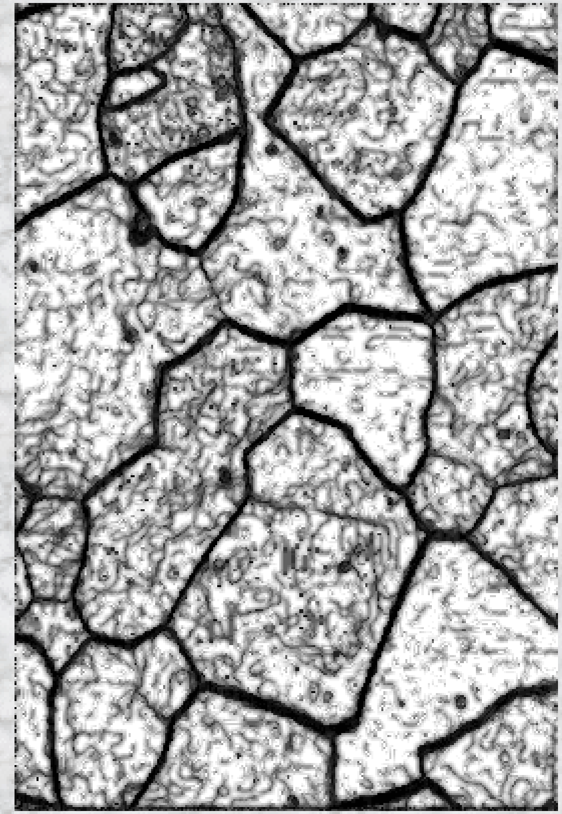

SIZE(*Evnbh*(Wnbh5x5,2,2))-filter

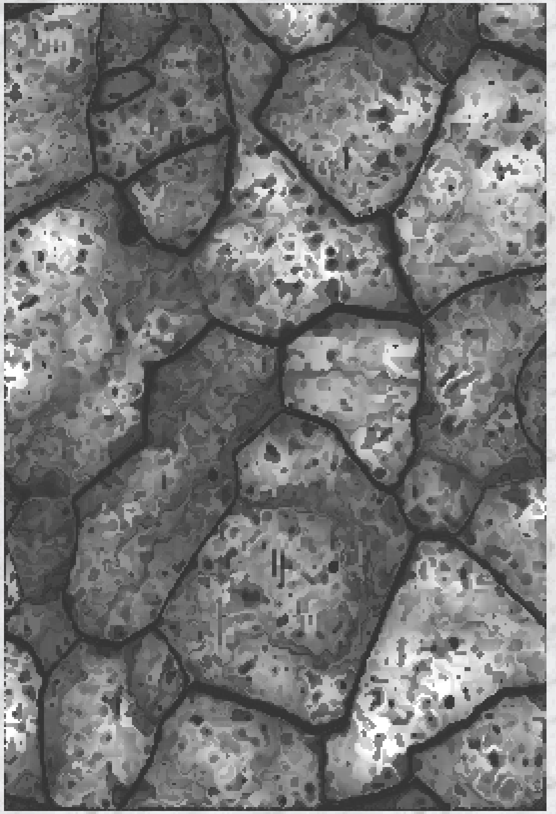

HIST(*W-nbh*)-filter

Local P-histogram equalization: color images (blind calibration of CCD-camera images)

IMAGE PROCESSING:
3-D VISUALIZATION

Redundancy of stereoscopic images

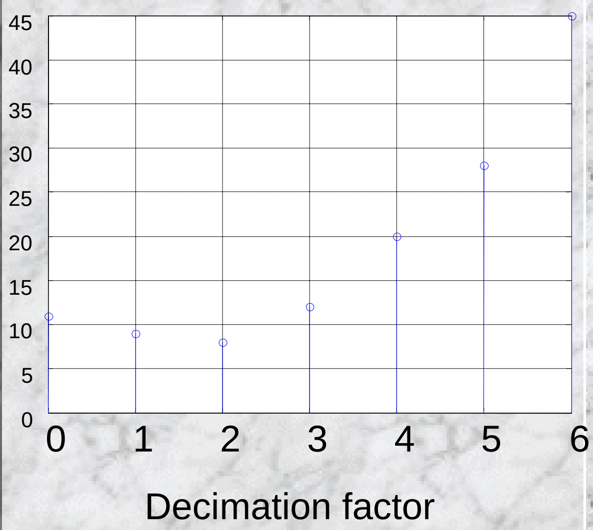

Standard deviation of parallax measuring versus image blur and decimation degree

Computer synthesis and display of stereoscopic images and video

Bahai garden, Haifa, Israel

Discobolus

Computer generated stereo from 2-D video

References

•L. Yaroslavsky, Digital Holography: 30 years later, IS&T/SPIE's 14th Ann. Symp. Electronic Imaging 2002, Science and Technology, Conference 4659A, "Practical Holography XVI", San Jose, CA, Proceedings of SPIE vol. 4659

•L. Yaroslavsky, Optical Transforms in Digital Holography, The Art and the Science of Holography, A tribute to Emmett Leith and Yuri Denisyuk, SPIE Press, Bellingham, Wa, 2004, pp. 45-60

•L.P. Yaroslavsky, B.-Z. Shaick, Transform Oriented Image Processing Technology for Quantitative Analysis of Fetal Movements in Ultrasound Image Sequences. In: Signal Processing IX. Theories and Applications, Proceedings of Eusipco-98,, S. Theodorisdis, I. Pitas, A. Stouraitis, N. Kalouptsidis, eds. Typorama Editions, 1998, p. 1745-1748

•L. Yaroslavsky, Optimal target location in color and multi component images, Asian Journal of Physics, Vol. 8, No 3 (1999) 355-369

•L. Yaroslavsky, Image Restoration, enhancement and target location with local adaptive filters, in:International Trends in Optics and Photonics, ICOIV, ed. by T.Asakura, Springer Verlag, 1999, pp. 111-127

•L. Yaroslavsky, A. Stainman, B. Fishbain, Sh. Gepstein, Processing and Fusion of Thermal and Video Sequences for Terrestrial Long Distance Observation Systems, ISIF, Seventh Intern. Conf. on Information Fusion (FUSION 2004), Stockholm, Sweden, 28 June - 1 July 2004 .

•L. Yaroslavsky, Boundary effect free and adaptive discrete sinc-interpolatioon, Applied Optics, 10 July 2003, v. 42, No. 20, p.4166-4175

•L. Yaroslavsky, F. Zhang, I. Yamaguchi, Point spread functions of digital reconstruction of digitally recorded holograms, In: Photonics Asia conference on Information Optics and Photonics Technology, 8-12 November 2004, Beijing, China

•L. Yaroslavsky, Nonlinear Filters for Image Processing in Neuromorphic Parallel Networks, Optical Memory and Neural Networks, v. 12, No. 1, 2003

•Ianir Ideses, Leonid Yaroslavsky, Three Methods that Improve Visual Quality of Color Anaglyphs, Journ. Pure &Appl. Optics, 7, (2005), p. 755-762

•L.P. Yaroslavsky, J. Campos, M. Espinola, I. Ideses, Redundancy of stereoscopic images: Experimental evaluation, Optics Express, v. 13, No. 26, Dec. 22, 2005, p. 10895

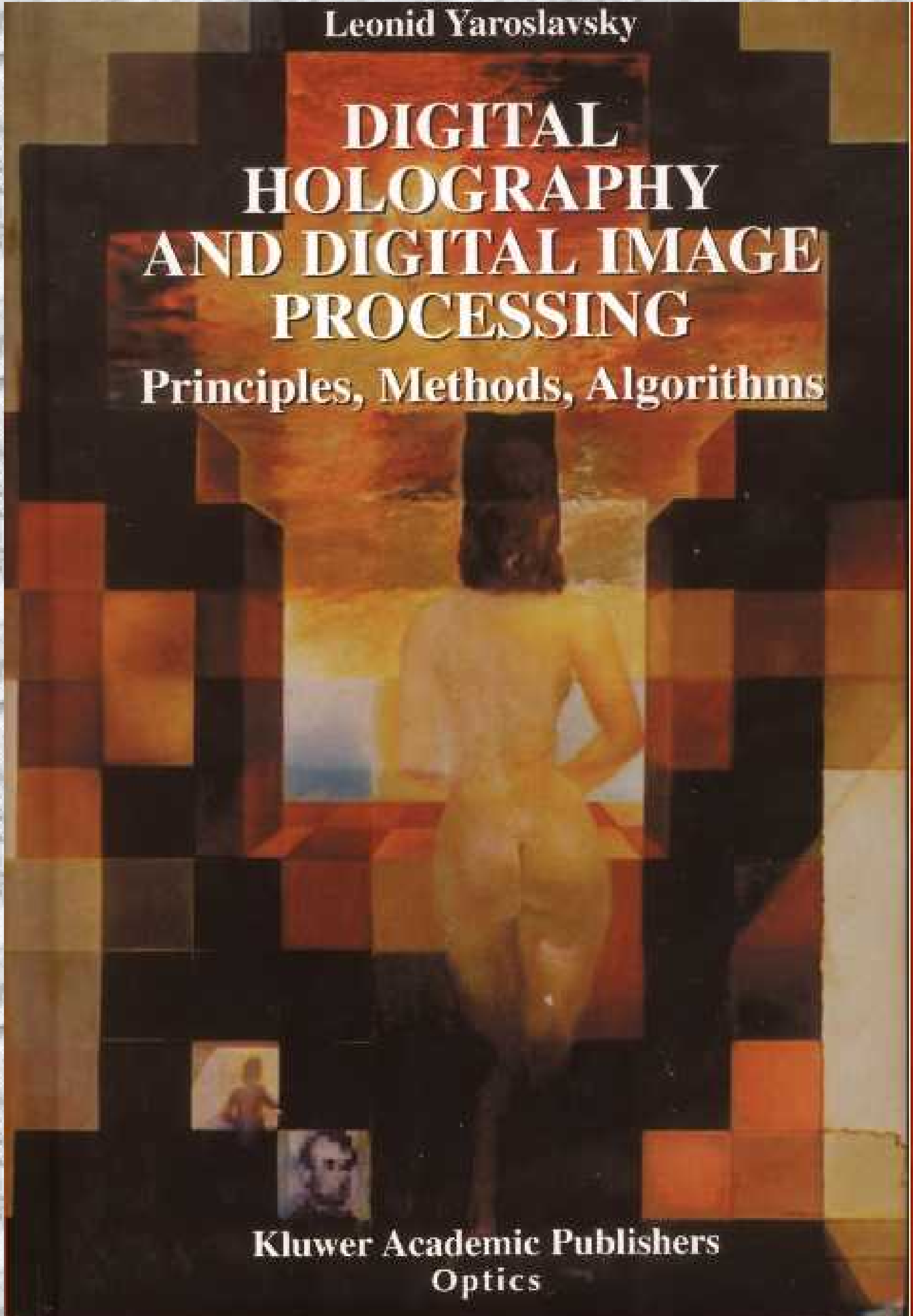

DIGITAL HOLOGRAPHY AND DIGITAL IMAGE PROCESSING
Principles, Methods, Algorithms

Digital holography and digital image processing are twins born by computer era. They share origin, theoretical base, methods and algorithms. The book describes these common fundamental principles, methods and algorithms including image and hologram digitization, data compression, digital transforms and efficient computational algorithms, statistical and Monte-Carlo methods, image restoration and enhancement, image reconstruction in tomography and digital holography, discrete signal resampling and image geometrical transformations, accurate measurements and reliable target localization in images, recording and reconstruction of computer generated holograms, adaptive and nonlinear filters for sensor signal perfecting and image restoration and enhancement.

DIGITAL HOLOGRAPHY AND DIGITAL IMAGE PROCESSING Principles, Methods, Algorithms combines theory, heavily illustrated practical methods and efficient computational algorithms, and is written for senior-level undergraduate and graduate students, researchers and engineers in optics, photonics, opto-electronics and electronic engineering.

ISBN 1-4020-7634-7

9 781402 076343

Kluwer Academic Publishers
1-4020-7634-7

Prof. L. Yaroslavsky,
Ph.D., Dr. Sc. Phys&Math,

Dept. of Interdisciplinary Studies, Faculty of Engineering, Tel Aviv University, Tel Aviv, Israel
www.eng.tau.ac.il/~yaro